Journal of Neuroinflammation

RESEARCH

Open Access

Therapeutic potential of targeting the IRF2/POSTN/Notch1 axis in nucleus pulposus cells for intervertebral disc degeneration

Daxue Zhu[1,2], Zhaoheng Wang[1,2], Shijie Chen[1,2], Yanhu Li[1,2] and Xuewen Kang[1,2*]

Abstract

Background Intervertebral disc degeneration (IDD) is a leading cause of low back pain, often linked to inflammation and pyroptosis in nucleus pulposus (NP) cells. The role of Periostin (POSTN) in IDD remains unclear.

Objective This study aims to investigate the influence of POSTN on pyroptosis and NLRP3 inflammasome activation in NP cells during IDD.

Methods IVD samples were collected from patients undergoing spinal surgery and classified according to the Pfirrmann grading system. Human NP cells were cultured and treated with IL-1β to induce a pyroptotic phenotype. Western blotting, Immunofluorescence (IF), and immunohistochemistry (IHC) assessed the expression levels of relevant proteins. Chromatin immunoprecipitation (ChIP) and luciferase reporter assays verified the binding of IRF2 to the POSTN and GSDMD promoters and evaluated the activation levels of target genes. The severity of IDD was evaluated using MRI and histological analysis.

Results Deletion of POSTN significantly alleviated IDD by suppressing NLRP3 inflammasome activity and pyroptosis in NP cells. POSTN was found to aggravate NP cell pyroptosis by activating the NLRP3 inflammasome through the NF-κB (P65) and cGAS/STING signaling pathways. Furthermore, POSTN interacted with Notch1 to induce NLRP3 expression. IRF2 was identified as a regulator of POSTN at the transcriptional level, contributing to NLRP3 activation and NP cell pyroptosis. IRF2 also directly induced the transcriptional expression of GSDMD, mediating pyroptosis in NP cells. Chemical screening identified Glucosyringic acid (GA) as a direct inhibitor of POSTN, which delayed IDD progression.

Conclusion The study elucidates the pivotal role of POSTN in mediating NP cell pyroptosis through the NLRP3 inflammasome and highlights GA as a promising therapeutic candidate for IDD. These findings provide new insights into the molecular mechanisms of IDD and potential avenues for treatment.

Keywords Periostin, Interferon regulatory factor 2, Intervertebral disc degeneration, Nucleus pulposus, Pyroptosis, Notch1

*Correspondence:
Xuewen Kang
ery_kangxw@lzu.edu.cn
[1]Lanzhou University Second Hospital, 82 Cui-Ying-Men, Lanzhou 730030, PR China
[2]Key Laboratory of Orthopedic Disease of Gansu Province, Lanzhou University Second Hospital, Lanzhou 730030, PR China

Introduction

Intervertebral disc (IVD) degeneration (IDD) is a predominant cause of low back pain, noted for its high prevalence and substantial disability [1, 2]. The IVD structure comprises the endplate, annulus fibrosus (AF), and nucleus pulposus (NP). The NP and its constituent cells are crucial for preserving IVD health by cushioning the pressure between vertebral bodies and regulating the metabolic balance of the extracellular matrix (ECM) [3, 4]. Pyroptosis is a significant form of programmed cell death associated with inflammation, characterized by the activation of the inflammasome, formation of transmembrane pores, cell swelling, vesicle formation, and release of intracellular contents in response to stress [5, 6]. Recent studies have shown that the expression of pyroptosis-related proteins, such as NOD-like receptor family pyrin domain containing 3 (NLRP3), Caspase-1, and GSDMD, is significantly increased in IDD patients and rat models [7]. Exogenous stimuli such as lipopolysaccharide, interleukin (IL)-1β, and hydrogen peroxide can induce inflammatory responses through NLRP3 activation, mediating IDD [8, 9]. During IDD, the impairment of NP cells' biological functions, disruption of ECM homeostasis, and changes within the NP environment create a vicious cycle that accelerates disease progression [10, 11]. Notably, the activation of NLRP3 inflammasome and pyroptosis in NP cells exacerbates inflammatory responses, aggravates ECM imbalance, and leads to further decline of NP cells [12, 13]. However, the molecular mechanisms through which NP cell pyroptosis mediates IDD remain unclear and necessitate further investigation.

Periostin (POSTN), also referred to as osteoblast-specific factor 2, is located on chromosome 13q and is an adhesive protein consisting of 836 amino acids with a molecular weight ranging from 90 to 100 kDa [14, 15]. The structural characteristics of this protein include a hydrophilic C-terminus, an N-terminal signal peptide, a cysteine-rich region, and four homologous repeat sequences, with the diversity of the C-terminus primarily arising from proteolytic cleavage sites [16, 17]. As a secreted protein, POSTN binds to adiponectin on the cell membrane through its FAS-1 domain, thereby activating downstream signaling pathways [17]. To date, POSTN has been identified as a significant factor due to its aberrant expression in various diseases, including asthma [18, 19], osteoarthritis (OA) [20, 21], and tumors [22, 23]. Notably, evidence indicates that POSTN is upregulated in the synovial fluid of OA patients during the progression of the disease in vivo, and it facilitates the production of matrix metalloproteinases (MMPs) by OA-associated synovial cells [24, 25]. Furthermore, recent studies have demonstrated that POSTN activates the Wnt/β-catenin signaling pathway in chondrocytes, leading to cartilage degeneration [26, 27]. Moreover, our research team has previously demonstrated that the expression level of POSTN is significantly elevated and positively correlates with the severity of IDD [28]. Specifically, POSTN mediates the senescence, ECM metabolism, and apoptosis of NP cells by activating the Wnt/β-catenin and NF-κB (P65) signaling pathways [29, 30]. This suggests that POSTN may serve as a potential molecular target for the treatment of IDD.

In addition, POSTN negatively regulates the expression of peroxisome proliferator-activated receptor alpha (PPARα), thereby inducing cell pyroptosis, which is involved in renal and cardiac dysfunction associated with chronic kidney disease [31]. Furthermore, a recent study has demonstrated that POSTN exacerbates NLRP3 inflammasome-mediated pyroptosis in myocardial ischemia-reperfusion injury. However, silencing of POSTN suppressed the formation of the NLRP3 inflammasome in the myocardium; consequently, the levels of NLRP3, apoptosis-associated speck-like protein containing a caspase recruitment domain (ASC), cleaved Caspase-1, mature IL-1β, and IL-18 were significantly reduced [32]. Nevertheless, the specific mechanisms by which POSTN induces NLRP3 inflammasome activity and pyroptosis in NP cells remain unreported. Therefore, through genetic and pharmacological modulation of POSTN, we aimed to investigate the precise role and mechanism of POSTN in promoting NLRP3 inflammasome activity and pyroptosis in NP cells, as well as its involvement in the pathogenesis of IDD.

Our current study found that the expression levels of IRF2, POSTN, and Notch1 are elevated in degenerative NP tissue. Importantly, we demonstrated that the significant role of the IRF2/POSTN/Notch1-NLRP3 signal axis in IDD. Given that POSTN may play a crucial role in the pathological process of IDD, developing potential POSTN inhibitors is of great significance for effective treatment. We screened and identified a compound named Glucosyringic acid (GA), which can directly bind to POSTN and inhibit its expression. The results of both cellular and animal experiments are consistent, demonstrating that GA improves the pathological process of IDD by inhibiting POSTN expression. GA may serve as a potential candidate for the treatment of IDD, providing new options and prospects for drug therapy in IDD. In summary, this study investigates the molecular mechanisms by which POSTN induces NLRP3 inflammasome activation and pyroptosis in NP cells, aiming to identify effective treatment strategies for IDD based on these insights.

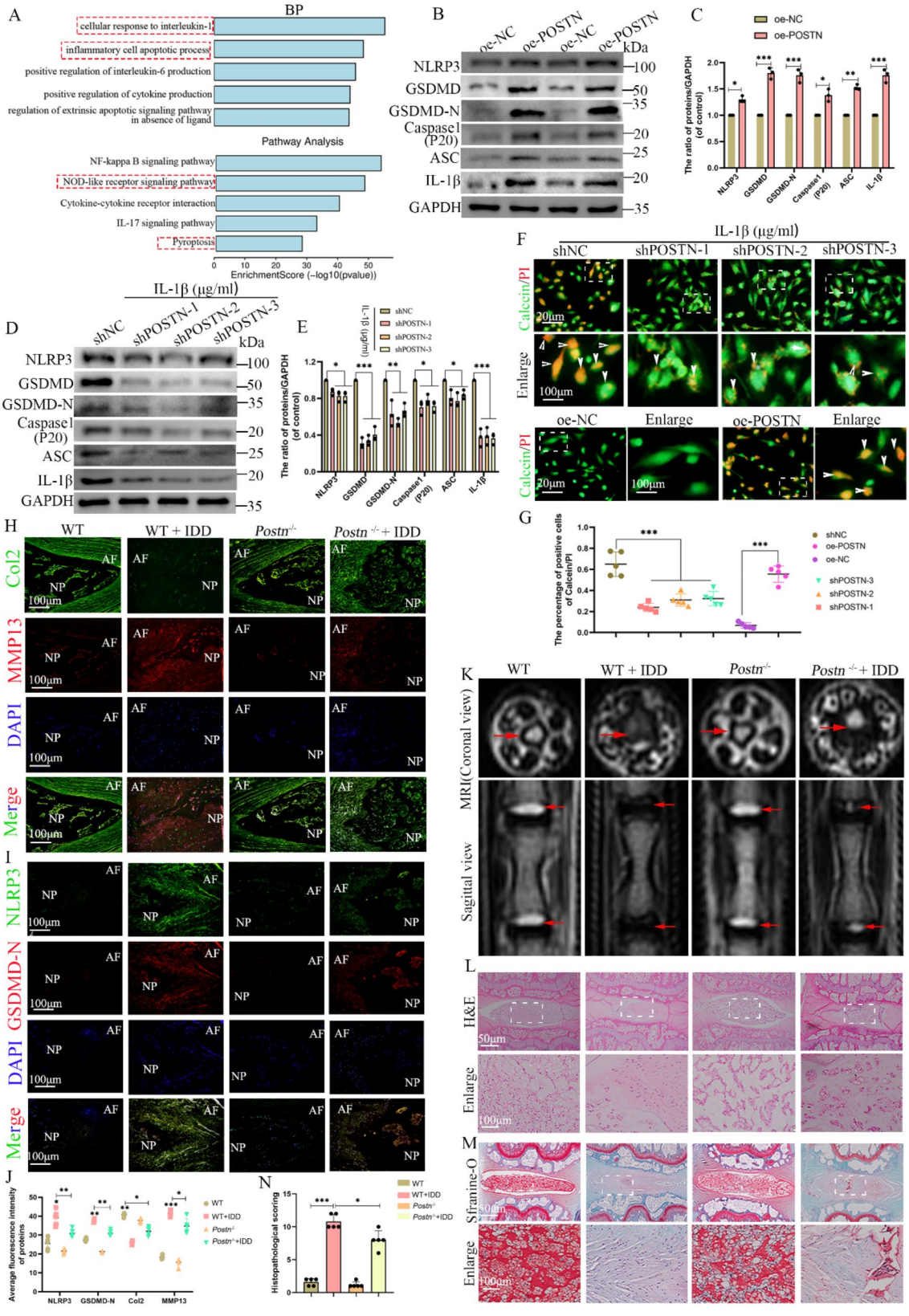

Fig. 1 (See legend on next page.)

(See figure on previous page.)

Fig. 1 POSTN deletion alleviates IDD by suppressing NLRP3 inflammasome activity and pyroptosis in NP cells. (**A**) GO and KEGG enrichment analysis of DEGs; (**B**-**E**) Western blotting analysis and quantitative assessment of NLRP3, GSDMD, GSDMD-N, Caspase-1 (P20), ASC, and IL-1β expression in various experimental groups; (**F**-**G**) Calcein/PI staining of NP cells and quantitative assessment across different experimental groups (scale bar = 20–100 μm); (**H**-**J**) IF staining and quantitative assessment of GSDMD-N, NLRP3, Col II, and MMP13 in different groups (scale bar = 100 μm); (**K**-**M**) MRI images, H&E, and Safranin-O/Fast Green staining of rat discs in different groups (scale bar = 50–100 μm); (**N**) Histopathological score was utilized to assess the extent of IDD in different groups. **P* < 0.05, ***P* < 0.01, ****P* < 0.001 compared to NC, the WT or WT + IDD groups. Values are presented as means ± SD from at least three independent experiments

Results

POSTN deletion alleviates IDD by suppressing NLRP3 inflammasome activity and pyroptosis in NP cells

To investigate the role of POSTN in IDD, we established NP cell lines with either POSTN overexpression or knockdown (shPOSTN-1, shPOSTN-2, and shPOSTN-3). The successful overexpression and knockdown of POSTN were confirmed through western blot analysis, demonstrating statistically significant differences ($P < 0.05$, Fig.S1A-D). Following this, we classified the NP cells overexpressing POSTN as the experimental group, while NP cells transfected with an empty vector served as the control group. To further elucidate the impact of POSTN on gene expression, we conducted high-throughput sequencing analysis on both groups, focusing on the identification of DEGs with thresholds set at $|\log2\ (FC)| \geq 1$ and $p < 0.05$. The transcriptome sequencing results revealed changes in gene expression profiles, with the DEGs illustrated in heat map and volcano map ($P < 0.05$, Fig.S1E-F). Subsequent GO and KEGG analyses indicated that these DEGs were predominantly linked to processes such as inflammatory cell apoptosis, the positive regulation of interleukin-6 production, and cellular responses to interleukin-1. Notably, KEGG pathway analysis underscored significant enrichment in pathways associated with NF-κB (P65) signaling, NOD-like receptor signaling, and pyroptosis ($P < 0.05$, Fig. 1A).

Based on these findings, we propose that POSTN may facilitate the progression of IDD by modulating the activity of the NLRP3 inflammasome and promoting pyroptosis in NP cells. To test this hypothesis, we assessed pyroptosis in NP cells with POSTN overexpression. Western blotting revealed elevated levels of NLRP3, GSDMD, GSDMD-N, ASC, IL-1β, and Caspase-1 (P20) in POSTN-overexpressing cells ($P < 0.05$, Fig. 1B-C). In contrast, POSTN knockdown cell lines exhibited reduced levels of GSDMD, GSDMD-N, Caspase-1 (P20), NLRP3, ASC, and IL-1β in the shPOSTN + IL-1β group compared to the IL-1β treatment group, indicating that POSTN knockdown mitigated IL-1β-induced NLRP3 inflammasome activation and pyroptosis in NP cells ($P < 0.05$, Fig. 1D-E). Calcein/PI staining revealed a significantly higher proportion of orange fluorescence in cells with POSTN overexpression, in contrast to a significantly lower proportion in cells with POSTN knockdown ($P < 0.05$, Fig. 1F and G).

To further explore the impact of POSTN knockout on pyroptosis in NP cells, we employed CRISPR/Cas9 technology to establish a *Postn*$^{-/-}$ rat model. The expression of POSTN mRNA in the POSTN knockout rat model was assessed using PCR gel electrophoresis. The results indicated that, compared to wild-type rats, POSTN expression was undetectable in the IVD of *Postn*$^{-/-}$ rats ($P < 0.05$, Fig.S1G-H). Furthermore, western blot and IHC analyses corroborated that POSTN protein was also absent in the IVD of the *Postn*$^{-/-}$ rats ($P < 0.05$, Fig.S1I-L). Then, an IDD model was created by puncturing the AF. Rats were divided into four groups: wild type (WT), WT + IDD, *Postn*$^{-/-}$, and *Postn*$^{-/-}$ + IDD. After 8 weeks, IF staining analyzed the expression of GSDMD-N, NLRP3, collagen II (Col II), and matrix metalloproteinase 13 (MMP13) in rat IVD tissue. Compared to the WT group, GSDMD-N, NLRP3, and MMP13 levels increased in the *Postn*$^{-/-}$ + IDD group, while Col II decreased. Conversely, compared to the WT + IDD group, GSDMD-N, NLRP3, and MMP13 levels decreased, and Col II levels increased following *POSTN* gene knockout ($P < 0.05$, Fig. 1H-J).

Additionally, MRI was used to assess IDD severity, and microstructural changes in the IVD were evaluated using H&E and Safranin-O/Fast Green staining. Histopathological score was employed for accurate IDD assessment. MRI results revealed a significant decrease in T2 signal in the IVD of the WT + IDD group, exhibiting the characteristic "black disc" phenomenon. In contrast, the T2 signal in the IVD of the *Postn-/-* + IDD group was somewhat enhanced, as indicated by the red arrow (Fig. 1K). H&E and Safranin-O/Fast Green staining confirmed disorganized AF structure, significant NP fibrosis, reduced ECM and NP cell numbers, and decreased disc height in the WT + IDD group, indicating severe degeneration. But in *Postn*$^{-/-}$ + IDD group, staining results showed improved AF structure, reduced NP fibrosis, increased NP cell and ECM numbers, and greater intervertebral space height compare to WT + IDD group (Fig. 1L-M). Histopathological score indicated that the *Postn*$^{-/-}$ + IDD group had higher scores than the WT group but lower than the WT + IDD group ($P < 0.05$, Fig. 1N). Collectively, these findings demonstrate that POSTN knockout effectively inhibits IDD progression by suppressing NLRP3 inflammasome activity and pyroptosis in NP cells.

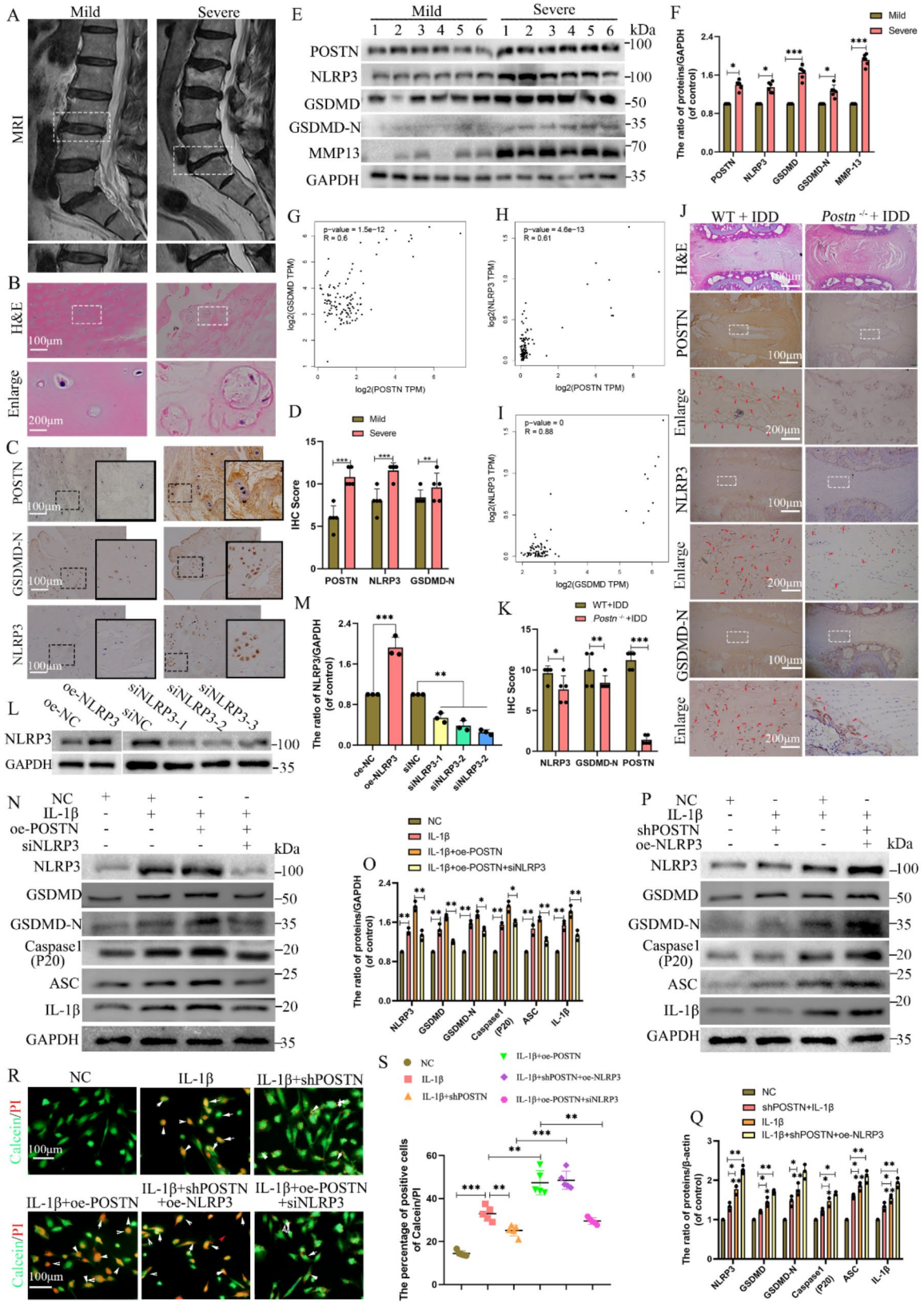

Fig. 2 (See legend on next page.)

(See figure on previous page.)

Fig. 2 POSTN aggravate GSDMD induced NP cells pyroptosis by activating NLRP3 inflammasome. (**A**) MRI images of the spine obtained from patients with mild and severe IDD; (**B**) H&E staining of IVDs derived from patients with mild and severe IDD (scale bar = 100 μm); (**C**-**D** and **J**-**K**) IHC staining of POSTN, NLRP3, and GSDMD-N and quantitative analysis in different groups(scale bar = 50–100 μm); (**E**-**F**) Western blotting of POSTN, MMP13, NLRP3, GSDMD, and GSDMD-N and quantitative analysis in mild and severe degenerative IVDs; (**G**-**I**) Analysis of the expression correlation between POSTN and NLRP3($R = 0.61$, $P < 0.001$), POSTN and GSDMD($R = 0.6$, $P < 0.001$), and GSDMD and NLRP3($R = 0.88$, $P < 0.001$) through the GEPIA database; (**L**-**Q**) Western blotting of NLRP3, GSDMD, GSDMD-N, Caspase-1(P20), ASC, and IL-1β and quantitative analysis in different groups; (**R**-**S**) Calcein/PI staining of NP cells and quantitative assessment in different experimental groups (scale bar = 100 μm). $^{*}P < 0.05$, $^{**}P < 0.01$, $^{***}P < 0.001$ versus Mild or NC. The values are presented as the means ± SD from at least three independent experiments

POSTN aggravate GSDMD induced NP cells pyroptosis by activating NLRP3 inflammasome

To explore whether POSTN-mediated pyroptosis in NP cells occurs through NLRP3 inflammasome activation, we examined the expression levels of POSTN, NLRP3, and GSDMD-N in IVD tissues from patients with IDD. MRI analysis showed significant reductions in T2 signal and disc height in moderate degenerative discs compared to mild degenerative discs (Fig. 2A). H&E staining revealed severe fibrosis, decreased ECM, and increased aggregation of NP cells in severely degenerated tissues (Fig. 2B). IHC confirmed that expression levels of POSTN, NLRP3, and GSDMD-N were significantly elevated in the disc tissues of patients with severe degeneration ($P < 0.05$, Fig. 2C-D), consistent with western blotting results ($P < 0.05$, Fig. 2E-F). Correlation analyses indicated a positive relationship among POSTN, NLRP3, and GSDMD-N ($P < 0.05$, Fig. 2G-I), suggesting that POSTN may mediate NP cell pyroptosis by regulating GSDMD expression through NLRP3 activation.

To validate our hypothesis, we established IDD models in WT and *Postn*$^{-/-}$ rats and used IHC to detect expression differences of NLRP3 and GSDMD-N between the two groups. Results showed significantly reduced levels of NLRP3 and GSDMD-N in the *Postn*$^{-/-}$ + IDD group compared to the WT + IDD group ($P < 0.05$, Fig. 2J-K). In addition, we knocked down or overexpressed NLRP3 in NP cells using plasmid or lentivirus-mediated transfection, confirming transfection efficiency via western blotting ($P < 0.05$, Fig. 2L-M). Following this, we constructed NP cells with either POSTN knockdown and NLRP3 overexpression or POSTN overexpression and NLRP3 knockdown. We evaluated cell pyroptosis through western blotting and Calcein/PI staining. In NP cells overexpressing POSTN, levels of NLRP3, GSDMD, GSDMD-N, Caspase-1 (P20), ASC, and IL-1β were significantly increased. However, when small interfering RNA (siNLRP3) was used to inhibit NLRP3 expression, the promoting effect of POSTN overexpression on GSDMD, GSDMD-N, ASC, Caspase-1 (P20), and IL-1β levels was abolished ($P < 0.05$, Fig. 2N-O). Moreover, after NLRP3 overexpression, the inhibitory effect of POSTN knockdown on GSDMD-mediated NP cell pyroptosis was reversed ($P < 0.05$, Fig. 2P-Q). Finally, Calcein/PI staining further confirmed that POSTN promotes GSDMD-mediated cell pyroptosis in an NLRP3-dependent manner ($P < 0.05$, Fig. 2R-S).

POSTN induces NLRP3 expression through the NF-κB (P65) and cGAS/STING signaling pathways

We conducted transcriptome sequencing on NP cells overexpressing POSTN, followed by KEGG enrichment analysis of DEGs. This analysis revealed significant enrichment in the NF-κB (P65) and NOD-like receptor signaling pathways ($P < 0.05$, Fig. 1D). Previous studies have highlighted the roles of the NF-κB (P65) and cGAS/STING pathways in IDD pathogenesis [33, 34], and activation of the cGAS-STING-NLRP3 axis has been linked to pyroptosis in NP cells [35]. Our earlier work confirmed that POSTN activates the NF-κB (P65) pathway, mediating inflammatory responses in NP cells [36]. Thus, we hypothesize that POSTN activates the NLRP3 inflammasome through the NF-κB (P65) and cGAS/STING pathways; however, the specific interactions between POSTN and the cGAS/STING pathway require further investigation.

To assess the activity of the NF-κB (P65) and cGAS/STING pathways, we analyzed human IVD tissues with varying degrees of degeneration. Western blotting results indicated increased activity of both pathways in severely degenerated tissues ($P < 0.05$, Fig. 3A-B), which was corroborated by IHC staining ($P < 0.05$, Fig. 3E-F). Additionally, we established a rat model of IDD, confirming elevated NF-κB (P65) and cGAS/STING activity ($P < 0.05$, Fig. 3C-D). Next, we explored the relationship between POSTN and the NF-κB (P65) and cGAS/STING pathways through knockdown and overexpression experiments. Western blotting revealed that suppression of POSTN decreased levels of phosphorylated P65 (p-P65), cGAS, and STING, while overexpression increased these levels ($P < 0.05$, Fig. 3G-J). In WT and *Postn*$^{-/-}$ rat IDD models, IF staining showed that p-P65 and STING levels in the *Postn*$^{-/-}$ + IDD group were lower than that in the WT + IDD group ($P < 0.05$, Fig. 3K-L). These results suggest that POSTN activates both the NF-κB (P65) and cGAS/STING pathways, while its suppression diminishes their activity.

Finally, we investigated whether POSTN activates the NLRP3 inflammasome via these pathways. Under IL-1β treatment, POSTN knockdown reduced NF-κB (P65) signaling and NLRP3 expression. Reactivation

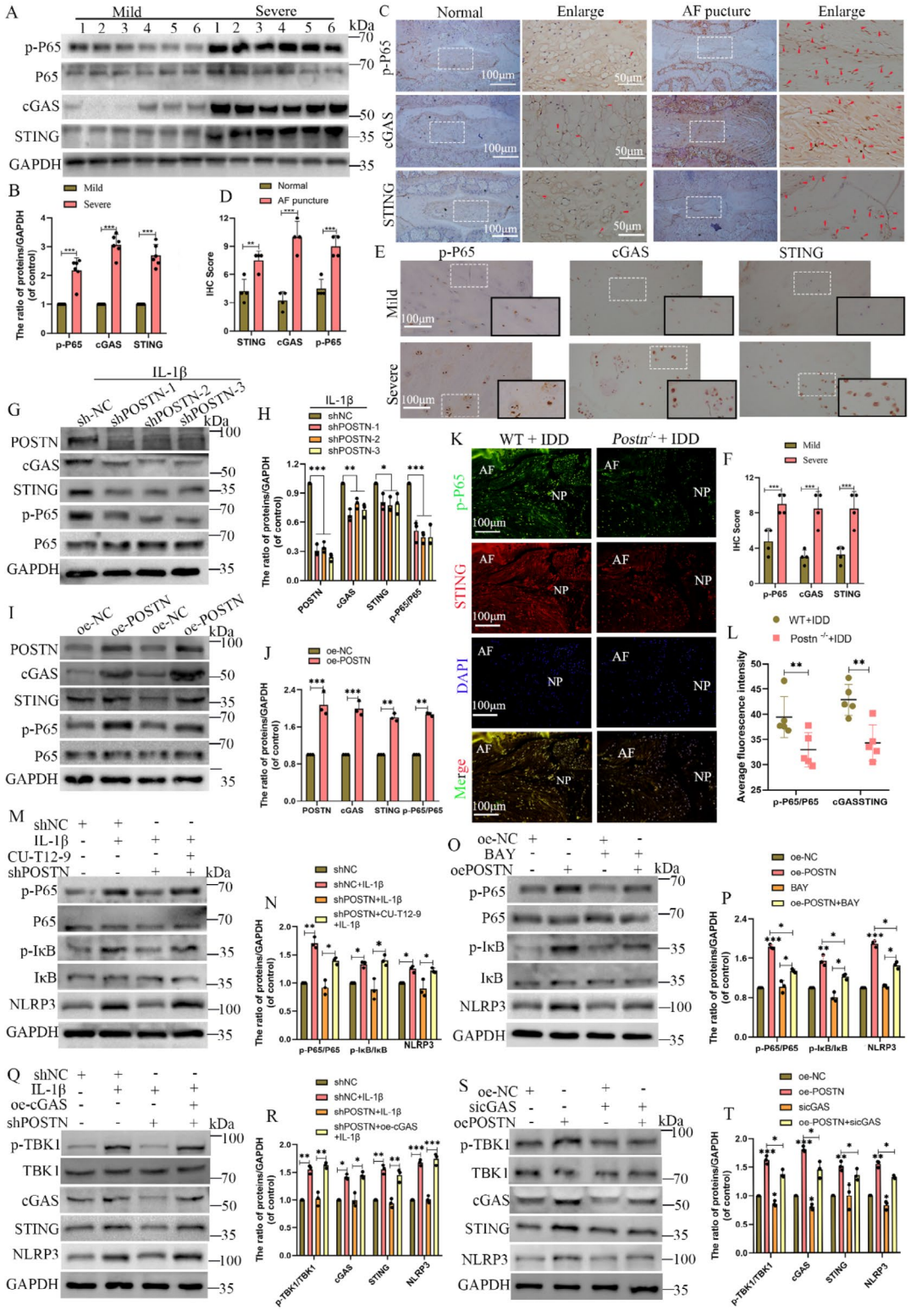

Fig. 3 POSTN induces NLRP3 expression through the NF-κB (P65) and cGAS/STING signaling pathways. (**A**-**B**) Western blotting of p-P65, P65, cGAS, and STING and quantitative analysis in mild and severe degenerative IVDs; (**C**-**F**) IHC staining of p-P65, cGAS, and STING and quantitative analysis in different groups (scale bar = 50–100 μm); (**G**-**J** and **M**-**T**) Western blotting of p-P65, P65, p-IκB, IκB, p-TBK1, TBK1, cGAS, STING, and NLRP3 and quantitative analysis in different groups. (**K**-**L**) IF staining of p-P65 and STING and quantitative assessment in different groups (scale bar = 100 μm). *$P < 0.05$, **$P < 0.01$, ***$P < 0.001$ versus Mild, WT + IDD or NC. The values are presented as the means ± SD from at least three independent experiments

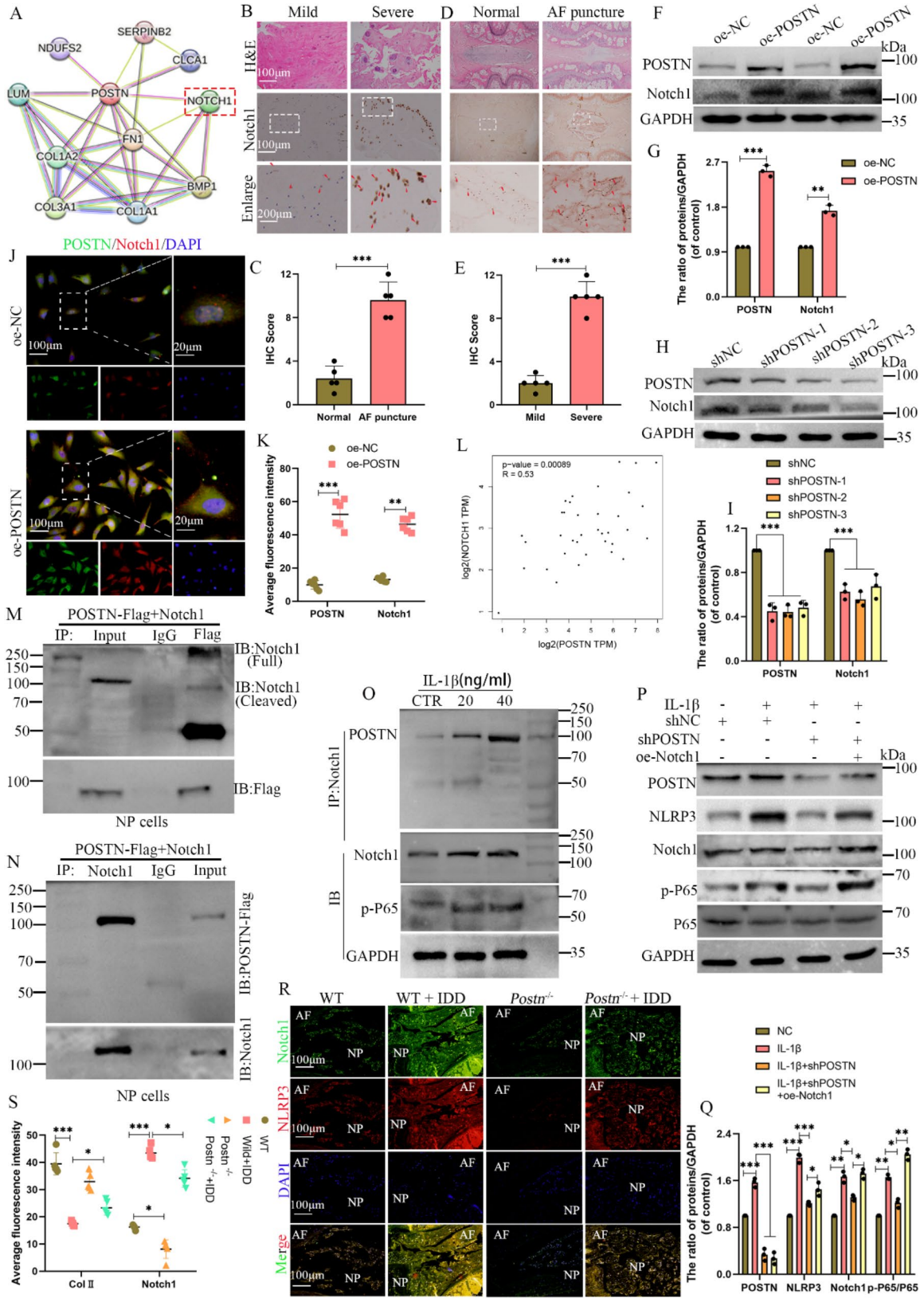

Fig. 4 (See legend on next page.)

(See figure on previous page.)

Fig. 4 POSTN interacts with Notch1 to activate the NF-κB (P65) pathway and induce the NLRP3 expression in NP cells. (**A**) The String database was employed to identify proteins that interact with POSTN; (**B**-**E**) IHC staining of Notch1 and quantitative analysis in different groups (scale bar = 100–200 μm); (**F**-**I** and **P**-**Q**) Western blotting of POSTN, Notch1, p-P65, NLRP3, and P65 and quantitative analysis in different groups; (**J**-**K**) IF staining of POSTN and Notch1 and quantitative assessment in different groups (scale bar = 100 μm–20 μm); (**L**) Analysis of the expression correlation between POSTN and Notch1 through the GEPIA database ($R = 0.53$, $P < 0.001$); (**M**-**N**) Co-IP assay between POSTN and Notch1 in the NP cells; (**O**) Co-IP assay of Notch1 and western blotting of Notch1and p-P65 in different groups; (**R**-**S**) IF staining of NLRP3 and Notch1 and quantitative assessment in rat IVD of different groups (scale bar = 100 μm). *$P < 0.05$, **$P < 0.01$, ***$P < 0.001$ versus Mild or NC or WT. The values are presented as the means ± SD from at least three independent experiments

of NF-κB (P65) using the agonist CU-T12-9 restored NLRP3 expression ($P < 0.05$, Fig. 3M-N). Conversely, POSTN overexpression significantly enhanced NF-κB (P65) signaling and NLRP3 expression, while inhibition of NF-κB (P65) with BAY markedly reduced NLRP3 levels ($P < 0.05$, Fig. 3O-P). We also investigated the cGAS/STING pathway to confirm POSTN's regulatory role on NLRP3 expression. Inhibiting cGAS while overexpressing POSTN decreased NLRP3 levels, whereas inhibiting POSTN while overexpressing cGAS increased NLRP3 expression ($P < 0.05$, Fig. 3Q-T). In summary, our findings indicate that POSTN activates the NLRP3 inflammasome by enhancing the activity of the NF-κB (P65) and cGAS/STING signaling pathways.

POSTN interacts with Notch1 to activate the NF-κB (P65) pathway and induce the NLRP3 expression in NP cells

Previous studies have shown that POSTN modulates NLRP3 expression via the NF-κB (P65) pathway. To elucidate the molecular mechanism underlying this activation, we utilized the STRING database to identify interacting proteins, highlighting Notch1 as a significant candidate (Fig. 4A). Research indicates that NLRP3 inflammasome-mediated cell pyroptosis affects angiogenesis in a Notch1-dependent manner [37]. Furthermore, inhibiting the Notch1 pathway can reduce renal inflammation and podocyte damage associated with NLRP3 activation [38]. Notch1 also interacts with various growth and apoptosis-related pathways, including NF-κB (P65) [39]. Thus, we hypothesize that POSTN activates the NF-κB pathway through Notch1, leading to NLRP3 expression.

To test this hypothesis, we first examined Notch1 expression in IVD tissues from patients with IDD and in rat models of IDD. IHC analyses revealed significant upregulation of Notch1 in IDD tissues ($P < 0.05$, Fig. 4B-E). We then assessed the effects of POSTN knockdown and overexpression on Notch1 levels. Western blotting demonstrated that POSTN overexpression increased Notch1 expression, while knockdown decreased it ($P < 0.05$, Fig. 4F-I). IF staining confirmed these findings, showing co-localization of POSTN and Notch1 ($P < 0.05$, Fig. 4J-K). Correlation analysis indicated a significant positive relationship between their expression levels ($R = 0.57$, $P < 0.001$, Fig. 4L). Co-IP assays further confirmed a direct interaction between POSTN and Notch1 in NP cells ($P < 0.05$, Fig. 4M-N).

Next, we evaluated the impact of the POSTN-Notch1 interaction on the NF-κB (P65) pathway. NP cells were treated with varying concentrations of IL-1β (0, 20, and 40 ng/ml). Western blotting revealed increased Notch1 and phosphorylated P65 (p-P65) levels with higher IL-1β concentrations. Co-IP assays indicated a corresponding increase in POSTN expression with escalating IL-1β levels ($P < 0.05$, Fig. 4O). To determine if POSTN mediates NLRP3 expression through the NF-κB (P65) pathway via Notch1, we established four experimental groups: negative control (NC), NC + IL-1β, shPOSTN + IL-1β, and shPOSTN + IL-1β + oe-Notch1. Western blotting showed that POSTN knockdown significantly reduced NF-κB (P65) activation, Notch1, and NLRP3 expression induced by IL-1β. Conversely, simultaneous knockdown of POSTN and overexpression of Notch intracellular domain (NICD) restored NF-κB (P65) pathway activity and NLRP3 expression ($P < 0.05$, Fig. 4P-Q).

In vivo validation involved a *Postn*$^{-/-}$ rat model, categorized into four groups: WT, WT + IDD, *Postn*$^{-/-}$, and *Postn*$^{-/-}$ + IDD. IF staining observations in rat IVD tissue indicated a decrease in Notch1 and NLRP3 expression in the *Postn*$^{-/-}$ group compared to the WT group, while Notch1 and NLRP3 expression increased in both the WT + IDD and *Postn*$^{-/-}$ + IDD groups, with a subsequent decrease in Notch1 and NLRP3 expression in the *Postn*$^{-/-}$ + IDD group relative to the WT + IDD group ($P < 0.05$, Fig. 4R-S). These results indicate that Notch1 is upregulated in IDD and that inhibiting POSTN reduces Notch1 levels. Furthermore, these findings suggest that POSTN may activate the NF-κB (P65) pathway to regulate NLRP3 expression, potentially through its interaction with Notch1.

IRF2 regulates POSTN at the transcriptional level to induce NLRP3 expression in NP cells

To explore the upstream mechanisms by which POSTN mediates pyroptosis in NP cells, we sought to identify transcription factors that influence POSTN gene expression. Utilizing the HumanTFDB and hTFtarget databases, we identified 321 potential transcription factors. We then screened 1,241 genes associated with pyroptosis through GeneCards, CTD, and DisGeNET databases. Venn diagram analysis revealed four transcription factors: IRF2, JUND, RUNX3, and STAT3 that regulate POSTN expression and are linked to cell pyroptosis (Fig. 5A). Further

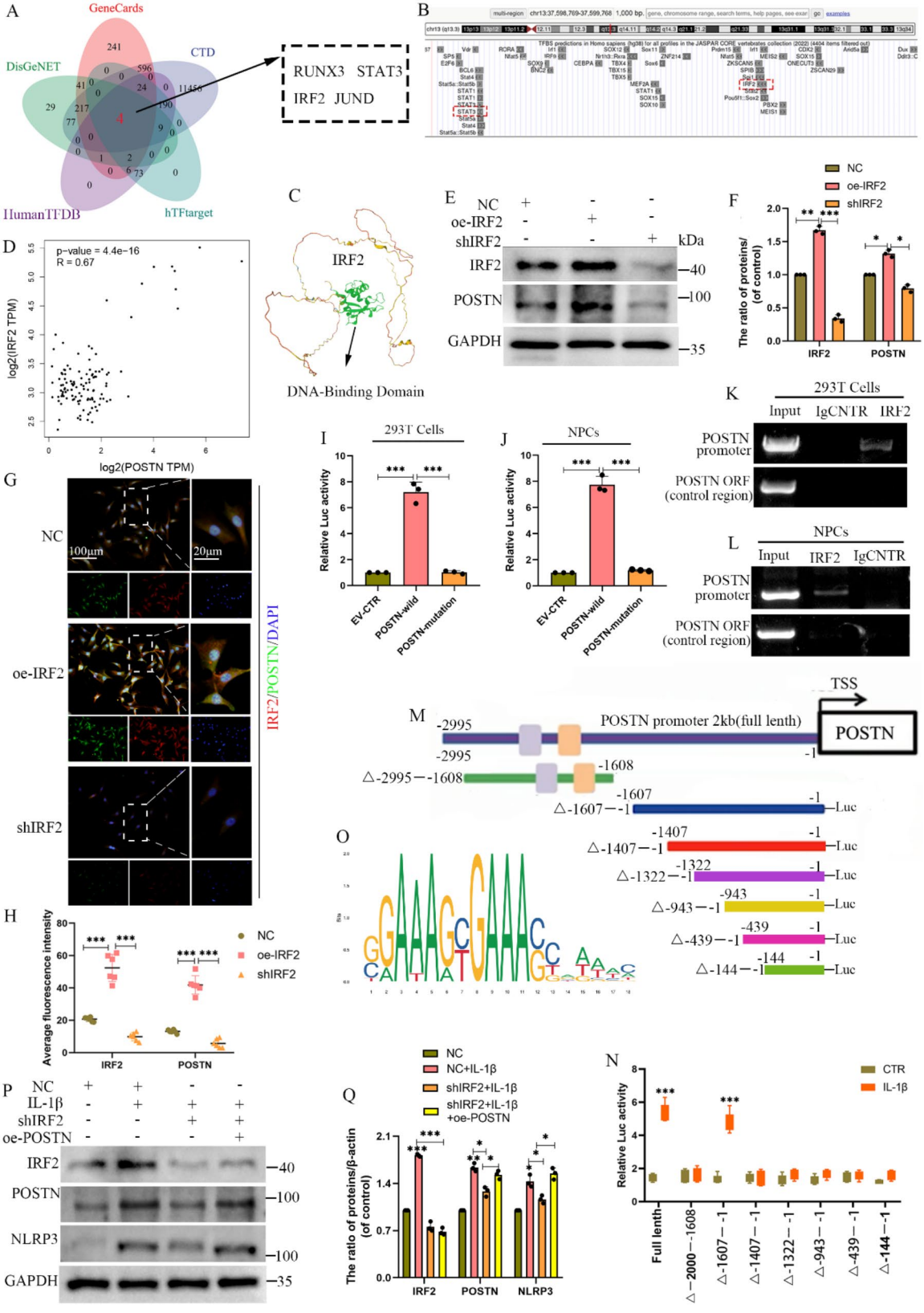

Fig. 5 (See legend on next page.)

(See figure on previous page.)

Fig. 5 IRF2 regulates POSTN at the transcriptional level to induce NLRP3 expression in NP cells. (**A**) Venn diagrams of the HumanTFDB, hTFtarget, GeneCards, CTD, and DisGeNET databases identify potential transcription factors that not only regulate POSTN expression but are also linked to cell pyroptosis; (**B**) The JASPAR and UCSC databases were used to predict transcription factors for POSTN; (**C**) The protein structure of IRF2, highlighting the presence of a DNA-binding domain; (**D**) Analysis of the expression correlation between IRF2 and POSTN through the GEPIA database ($R = 0.67$, $P < 0.001$); (**E**-**F** and **P**-**Q**) Western blotting analysis of IRF2, POSTN, and NLRP3 with quantitative analysis across different groups; (**G**-**H**) IF staining and quantitative assessment of IRF2 and POSTN in different groups (scale bar = 100 μm–20 μm); (**I**-**J**) Dual-luciferase reporter assay demonstrating that POSTN is a target of IRF2 in both 293T and NP cells; (**K**-**L**) ChIP-PCR gel electrophoresis analysis of IRF2 and the POSTN promoter revealing that IRF2 is capable of binding to the POSTN promoter region in both 293T and NP cells; (**M**-**N**) Relative luciferase activity measured from seven different lengths of fragments of the POSTN promoter in NP cells; (**O**) Consensus DNA-binding motifs of IRF2 as predicted by the JASPAR database. *$P < 0.05$, **$P < 0.01$, ***$P < 0.001$ versus Mild or NC. The values are presented as means ± SD from at least three independent experiments

analysis using the JASPAR and UCSC databases identified IRF2 as a key candidate for POSTN regulation (Fig. 5B), with its structure and binding sites illustrated in Fig. 5C.

Correlation analysis via the GEPIA database showed a significant positive correlation between IRF2 and POSTN expression ($R = 0.67$, $P < 0.05$, Fig. 5D). To assess the regulatory role of IRF2, we performed knockdown and overexpression experiments, employing western blotting and IF staining. Results demonstrated that changes in POSTN expression corresponded to alterations in IRF2 levels ($P < 0.05$, Fig. 5E-H), suggesting that IRF2 might functions as a transcriptional regulator of POSTN. Both exogenous and endogenous dual-luciferase reporter assays showed that co-transfection of IRF2 with pGL3-POSTN significantly increased relative luciferase activity compared to controls ($P < 0.05$, Fig. 5I-J). Additionally, ChIP-PCR gel electrophoresis confirmed that IRF2 binds to the POSTN promoter region ($P < 0.05$, Fig. 5K-L). Although the specific binding motif remained unclear, we predicted potential binding sites using the JASPAR database, identifying six sites with a relative score > 0.7. Consequently, we amplified the full-length POSTN promoter region from – 2995 bp to the transcription start site, as well as seven shorter fragments, and co-transfected these luciferase reporter gene plasmids into NP cells (Fig. 5M). Luciferase activity analysis, conducted 48 h post-transfection in the presence or absence of IL-1β, revealed a significant increase in luciferase activity within the – 1607 to -1407 region, indicating that this sequence contains the core transcriptional elements of the POSTN gene ($P < 0.05$, Fig. 5M-N). The predicted binding site from the JASPAR database, located between 1386 and 1403, has the nucleotide sequence: TGAAAAAGAAAGGAAATG (Fig. 5O). These findings confirm IRF2's role in promoting POSTN transcription and highlight its specific binding sites.

Finally, to determine if IRF2 activates the NLRP3 inflammasome in NP cells by regulating POSTN expression, we established four experimental groups: shNC, shNC + IL-1β, shIRF2 + IL-1β, and shIRF2 + oe-POSTN + IL-1β. Results indicated that IRF2 knockdown inhibited NLRP3 inflammasome activity induced by IL-1β, an effect that could be reversed by POSTN overexpression ($P < 0.05$, Fig. 5P-Q). These findings suggest that IRF2 activates the NLRP3 inflammasome through transcriptional regulation of POSTN.

IRF2 upregulation in IDD activates the NLRP3 inflammasome and induces pyroptosis in NP cells by regulating POSTN expression

Previous studies have established that IRF2 acts as a transcription factor for POSTN, playing a crucial role in the regulation of the NLRP3 expression. However, the expression of IRF2 in IDD has not been reported, and it remains unclear whether IRF2 mediates NLRP3 inflammasome activation and pyroptosis in NP cells. To investigate the expression pattern of IRF2 in IDD, we performed western blotting and IHC on mildly and severely degenerated IVD tissues. Western blotting results showed that the severely degenerated group had significantly higher levels of POSTN, NLRP3, and IRF2 than the mildly degenerated group ($P < 0.05$, Fig. 6A-B). IHC staining also confirmed increased expression of these proteins in the severely degenerated group ($P < 0.05$, Fig. 6C-D).

To further verify IRF2 expression, we established rat and cell models of IDD. In the rat IDD model, IHC staining revealed that POSTN, NLRP3, and IRF2 levels were significantly elevated in degenerated discs compared to normal rat IVDs ($P < 0.05$, Fig. 6E-F). In the cell model, we utilized two IDD models: an aging model and an IL-1β-induced model. In the aging model, SA-β-gal staining demonstrated significant aging of rat NP cells by the 8th generation, with severe aging by the 15th generation ($P < 0.05$, Fig.S2A-B). We selected the 2nd, 8th, and 15th generations to represent different degeneration levels. Western blotting revealed that as NP cell generations increased, P16 expression also increased, indicating elevated aging levels. Further analysis showed that IRF2, POSTN, and NLRP3 expression levels rose with cellular aging ($P < 0.05$, Fig.S2C-D). Additionally, in the IL-1β treatment model, RT-qPCR and western blotting demonstrated that the mRNA and proteins expression of IRF2, POSTN, and NLRP3 increased with higher IL-1β concentrations compared to the control group ($P < 0.05$, Fig. 6G-I). These findings suggest that IRF2 expression is elevated in IDD and may be closely linked to IDD progression.

We also explored the role of IRF2 in NP cell pyroptosis. Four experimental groups were established: control

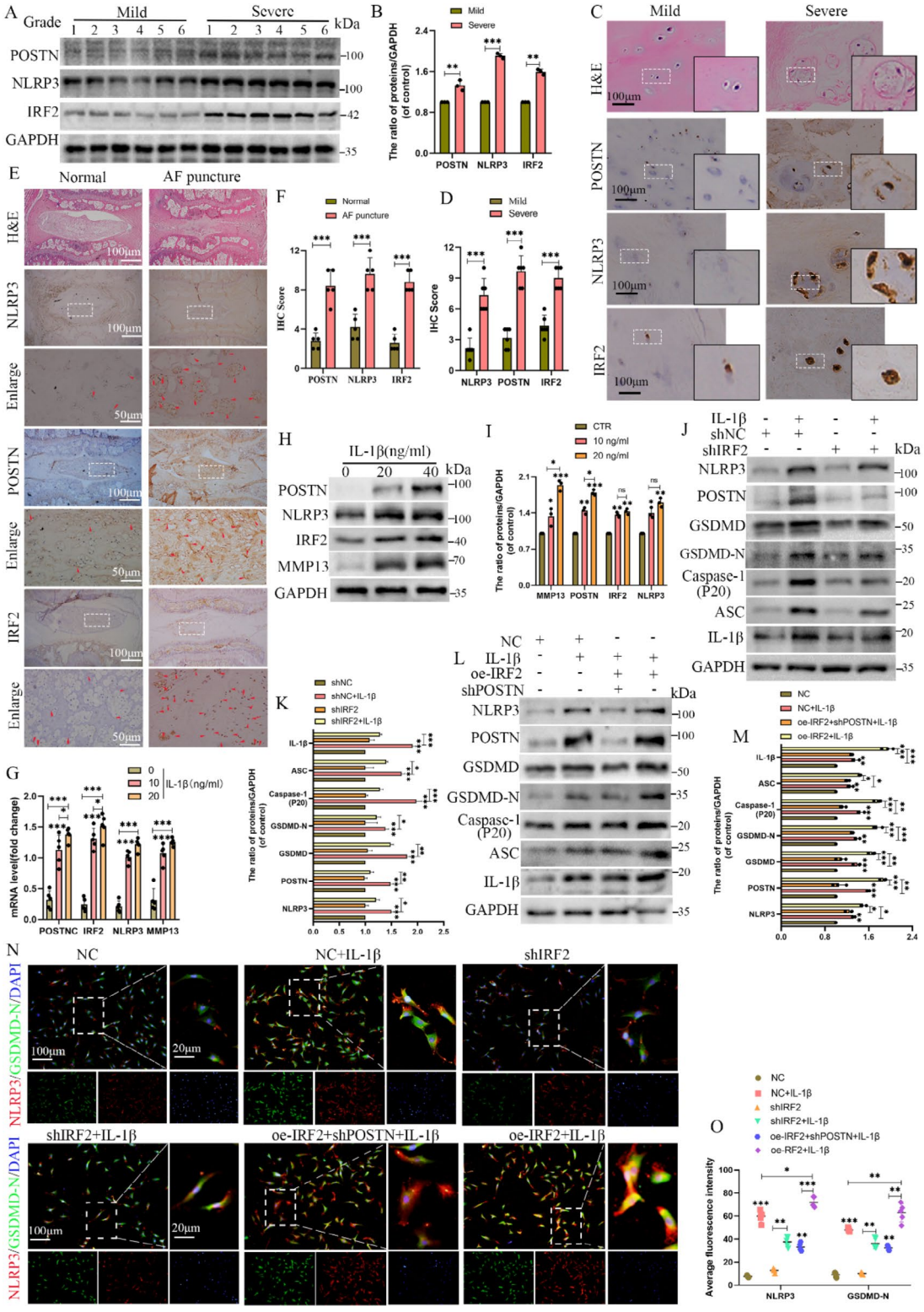

Fig. 6 IRF2 upregulation in IDD activates the NLRP3 inflammasome and induces pyroptosis in NP cells by regulating POSTN expression. (**A**-**B**) Western blotting of POSTN, IRF2, and NLRP3 and quantitative analysis in mildly and severely degenerated IVDs; (**C**-**F**) IHC staining of NLRP3, POSTN, and IRF2 and quantitative analysis (scale bar = 50–100 μm); (**G**) The mRNA expression of NLRP3, POSTN, and IRF2 in different groups; (**H**-**M**) Western blotting of NLRP3, POSTN, GSDMD, GSDMD-N, Caspase-1 P20), ASC, IRF2, MMP13, P16, and IL-1β and quantitative analysis in different groups; (**N**-**O**) IF staining of GSDMD-N and NLRP3 and quantitative assessment in different groups (scale bar = 100 μm–20 μm). *$P < 0.05$, **$P < 0.01$, ***$P < 0.001$ versus Mild or NC. The values are presented as the means ± SD from at least three independent experiments

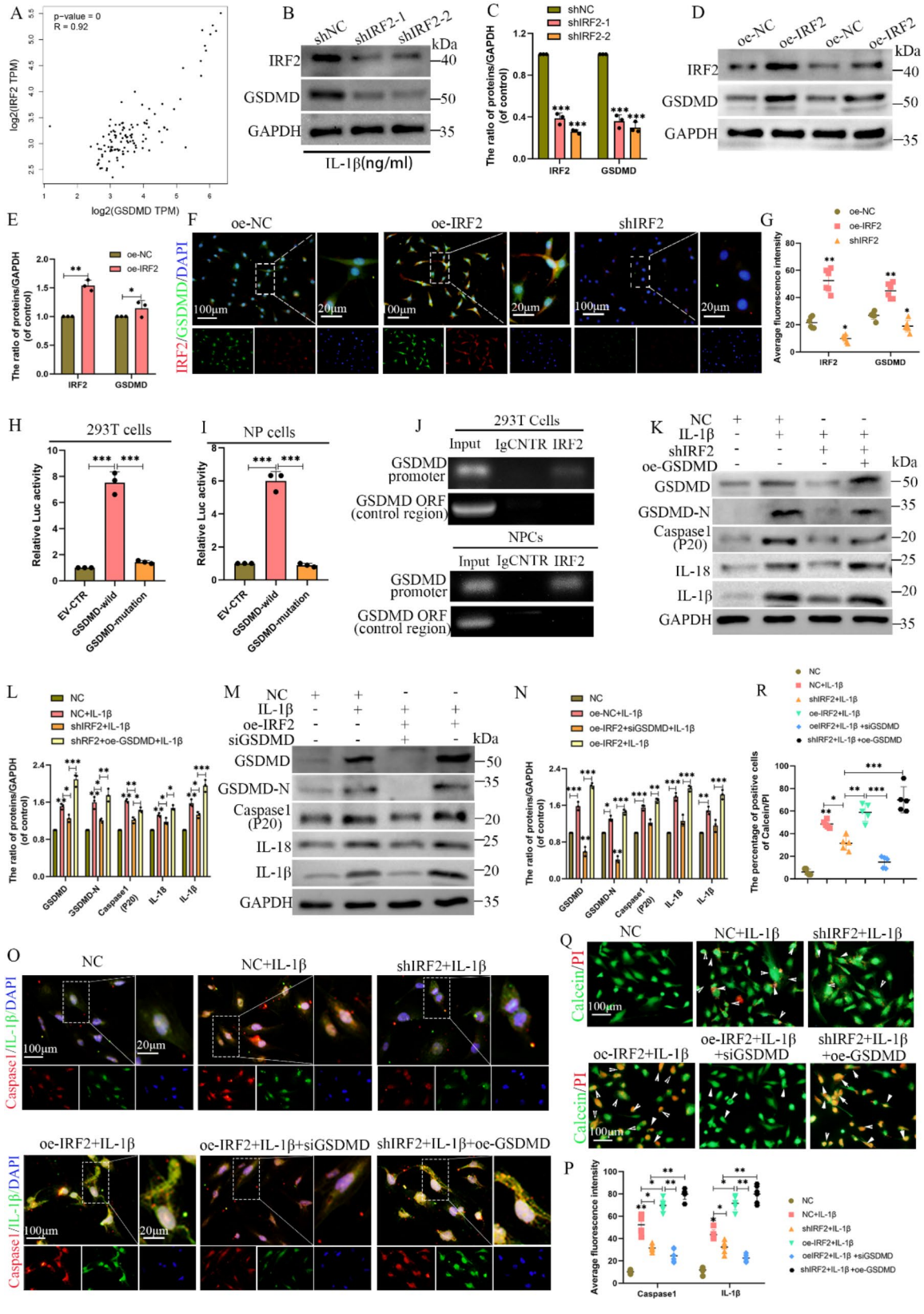

Fig. 7 (See legend on next page.)

(See figure on previous page.)

Fig. 7 IRF2 directly induced transcriptional expression of GSDMD, mediating pyroptosis in NP cells. (**A**) Analysis of the expression correlation between IRF2 and GSDMD through the GEPIA database ($R = 0.92$, $P < 0.001$); (**B**-**D** and **K**-**N**) Western blotting of IRF2, GSDMD, GSDMD-N, Caspase1(P20), IL-18, and IL-1β and quantitative analysis in different groups; (**F**-**G** and **O**-**P**) IF staining and quantitative assessment of IRF2, GSDMD, IL-1β, and Caspase1 in different groups (scale bar = 20–100 μm); (**H**-**I**) Dual-luciferase reporter assay showing that GSDMD was a target of IRF2 in 293T and NP cells; (**J**) ChIP-PCR gel electrophoresis analysis of IRF2 and the GSDMD promoter revealed that IRF2 is capable of binding to the GSDMD promoter region in both 293T and NP cells; (**Q**-**R**) Calcein/PI staining of NP cells and quantitative assessment in different experimental groups (scale bar = 100 μm). *$P < 0.05$, **$P < 0.01$, ***$P < 0.001$ versus NC. The values are presented as the means ± SD from at least three independent experiments

(shNC), shNC + IL-1β, shIRF2, and shIRF2 + IL-1β. Western blotting results indicated that IL-1β treatment increased the expression of POSTN, NLRP3, GSDMD, GSDMD-N, Caspase-1 (P20), ASC, and IL-1β in the shNC group. However, in the shIRF2 + IL-1β group, expression levels of these proteins were significantly reduced compared to the IL-1β group, suggesting that IRF2 knockdown can delay IL-1β-mediated activation of the NLRP3 inflammasome and pyroptosis in NP cells ($P < 0.05$, Fig. 6J-K). Furthermore, we manipulated the expression of IRF2 and POSTN to investigate whether IRF2 mediates NLRP3 inflammasome activation and pyroptosis in NP cells via POSTN regulation. Western blotting revealed that IRF2 overexpression significantly increased POSTN levels and enhanced IL-1β-induced NLRP3 activation and pyroptosis in NP cells, an effect reversed by POSTN knockdown ($P < 0.05$, Fig. 6L-M). In addition, IF staining for GSDMD-N, NLRP3, ASC, and Caspase1 staining results indicate that the knockdown of IRF2 alleviates IL-1β-induced NLRP3 inflammasome activation and NP cells pyroptosis, while overexpression of IRF2 exacerbates these effects ($P < 0.05$, Fig. 6N-O and Fig.S2E-F). Furthermore, Calcein/PI staining supported these findings ($P < 0.05$, Fig.S2G-H). These findings suggest that the role of IRF2 is mediated through the regulation of POSTN expression. Notably, while GSDMD expression also declined with POSTN knockdown, it did not decrease significantly as NLRP3 did, suggesting that IRF2 may employ additional mechanisms in mediating pyroptosis. Thus, we propose that IRF2 activates the NLRP3 inflammasome in NP cells by regulating POSTN expression, partially contributing to pyroptosis.

IRF2 directly induced transcriptional expression of GSDMD, mediating pyroptosis in NP cells

Our previous studies established that IRF2 is upregulated in IDD, acting as a transcription factor that regulates POSTN expression and contributes to IDD progression. Notably, while NLRP3 expression significantly decreased with POSTN knockdown during IRF2 overexpression, GSDMD and GSDMD-N levels also decreased, although not as markedly as NLRP3. This suggests that IRF2 may mediate pyroptosis through additional mechanisms. Literature indicates that IRF2 can function as a transcription factor for GSDMD [40], leading us to hypothesize that IRF2 directly modulates GSDMD transcription, thereby promoting cellular pyroptosis.

To support this hypothesis, we first analyzed the correlation between IRF2 and GSDMD expression using the GEPIA database, which revealed a strong positive correlation ($R = 0.92$, $P < 0.001$) (Fig. 7A). We then manipulated IRF2 levels through knockdown and overexpression, finding that IRF2 downregulation led to decreased GSDMD expression, while IRF2 overexpression increased GSDMD levels ($P < 0.05$, Fig. 7B-E). These results were further validated by IF staining of IRF2 and GSDMD ($P < 0.05$, Fig. 7F-G). Subsequently, we performed dual-luciferase reporter assays to investigate the binding of IRF2 to the GSDMD promoter. The results indicated a significant increase in luciferase activity in cells co-transfected with IRF2 and pGL3-GSDMD compared to controls ($P < 0.05$, Fig. 7H-I). Furthermore, ChIP-PCR gel electrophoresis confirmed IRF2's binding to the GSDMD promoter region, reinforcing its role in promoting GSDMD transcription in NP cells ($P < 0.05$, Fig. 7J).

To determine if IRF2 directly induces GSDMD transcription and mediates pyroptosis, we simultaneously knocked down IRF2 and overexpressed GSDMD. Western blotting showed that silencing IRF2 reduced IL-1β-induced expression of GSDMD, GSDMD-N, IL-18, and Caspase-1 (P20), effects that were reversed by GSDMD overexpression ($P < 0.05$, Fig. 7K-L). Conversely, IRF2 overexpression, coupled with GSDMD interference, exacerbated IL-1β-induced expression of these proteins, which was alleviated by disrupting GSDMD expression ($P < 0.05$, Fig. 7M-N). IF staining of IL-1β and Caspase-1 corroborated these findings ($P < 0.05$, Fig. 7O-P). Additionally, Calcein/PI staining confirmed that IRF2 silencing mitigated IL-1β-induced pyroptosis in NP cells, while GSDMD overexpression amplified it. Overexpression of IRF2 further intensified IL-1β-induced pyroptosis, which was reversed by GSDMD disruption ($P < 0.05$, Fig. 7Q-R). In conclusion, our results indicate that IRF2 directly binds to the GSDMD promoter, enhances its transcription, and plays a crucial role in mediating pyroptosis in NP cells.

Chemical screening and identification of GA, which directly targeted and inhibited POSTN expression to delay IDD

Given the critical role of POSTN in NP cell pyroptosis, previous studies in rats have shown that inhibiting POSTN expression effectively slows the progression of needle-induced IDD. Therefore, pharmacological inhibition of POSTN may offer a promising therapeutic

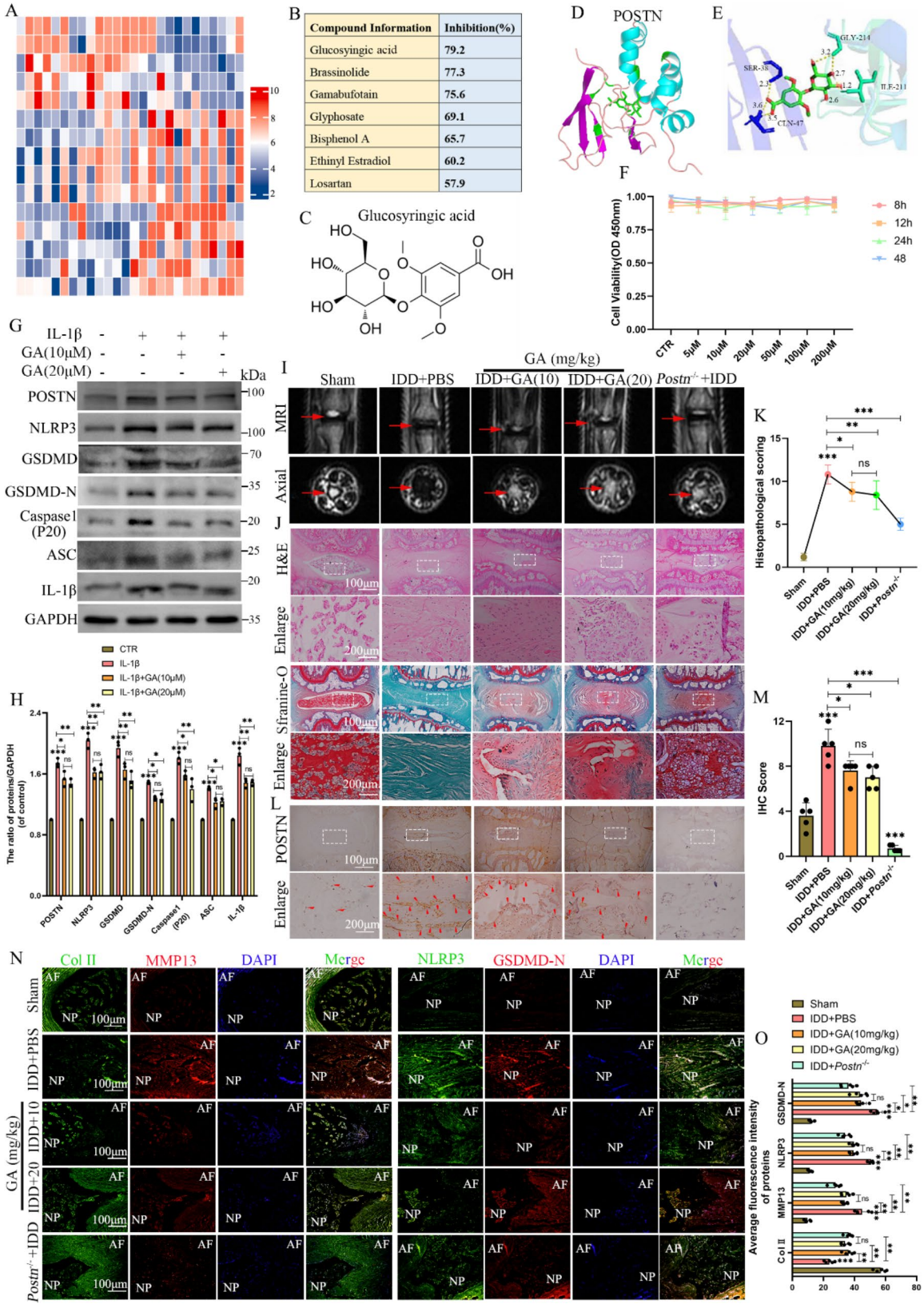

Fig. 8 (See legend on next page.)

(See figure on previous page.)

Fig. 8 Chemical screening and identification of GA, which directly targeted and inhibited POSTN expression to delay IDD. (**A**) Heatmap showing the effects of various compounds on the POSTN luciferase reporter gene activity; (**B**) Top seven compounds that inhibited POSTN luciferase reporter gene activity were shown; (**C**) The chemical structure of GA; (**D**-**E**) Molecular docking of GA to POSTN; (**F**) Effects of different doses of GA on the viability of NP cells; (**G**-**H**) Western blotting of POSTN, NLRP3, GSDMD, GSDMD-N, Caspase-1(P20), ASC, and IL-1β and quantitative analysis in different groups; (**I**-**J**) MRI images, H&E, and Safranin-O/fast green staining of rat discs in different groups (scale bar = 100–200 μm); (**K**) Histopathological score were utilized to assess the extent of IDD in different groups; (**L**-**M**) IHC staining of POSTN and quantitative analysis in different groups(scale bar = 100–200 μm); (**N**-**O**) IF staining and quantitative assessment of Col II, MMP13, NLRP3, and GSDMD-N and quantitative analysis in different groups (scale bar = 100 μm). *$P < 0.05$, **$P < 0.01$, ***$P < 0.001$ versus Sham or CTR. Values are presented as the mean ± SD from at least three independent experiments

strategy for managing IDD. To identify potential POSTN inhibitors, we constructed NP cells expressing a luciferase reporter gene driven by the POSTN promoter. From a library of approximately 390 natural product small molecules (Table.S3), GA was identified for its significant reduction in POSTN-luciferase activity ($P < 0.05$, Fig. 8A-B). The chemical structures of GA and protein structures of POSTN are illustrated in Fig. 8C and D. Molecular docking analysis revealed a direct interaction between GA and POSTN, with a binding energy of -6.6 kJ/mol (Fig. 8E), suggesting that GA could serve as a potential therapeutic agent for delaying IDD by inhibiting POSTN expression.

To evaluate the impact of GA on POSTN, we first assessed NP cell viability following GA treatment. CCK8 assays indicated minimal cytotoxicity of GA, even at higher concentrations, demonstrating favorable biocompatibility ($P < 0.05$, Fig. 8F). We then exposed NP cells to varying concentrations of GA (10 and 20 μM) to investigate its inhibitory effects on POSTN and its potential to mitigate IL-1β-induced NLRP3 inflammasome activation and pyroptosis in NP cells. Western blot analyses showed significant reductions in the expression of POSTN, NLRP3, GSDMD, GSDMD-N, Caspase-1 (P20), ASC, and IL-1β in the IL-1β + 10 μM and IL-1β + 20 μM groups compared to the IL-1β group, highlighting GA's pronounced inhibitory effect on POSTN expression and its beneficial impact on suppressing IL-1β-induced NLRP3 inflammasome activation and pyroptosis in NP cells ($P < 0.05$, Fig. 8G-H). The results were further validated by IF staining of NLRP3, GSDMD, ASC, and Caspase-1 ($P < 0.05$, Fig. S3A-C and E). Furthermore, Calcein/PI staining confirmed that GA effectively mitigates the activation of the NLRP3 inflammasome and the pyroptosis in NP cells induced by IL-1β ($P < 0.05$, Fig. S3D and F).

Furthermore, we assessed GA's therapeutic potential in managing IDD in rats. The study design included five groups: Sham, IDD + PBS, IDD + GA (10 mg/kg), IDD + GA (20 mg/kg), and IDD + *Postn*$^{-/-}$ (positive control). MRI was employed to evaluate the extent of IDD following different interventions. Results demonstrated that both the GA treatment and IDD + *Postn*$^{-/-}$ groups exhibited reduced water content and disc height compared to the Sham group, but showed increased water content and disc height relative to the IDD + PBS group (Fig. 8I). Histological staining of NP tissue using H&E and Safranin O-Fast Green revealed reduced structural disruption and fibrosis in the lumbar discs of the GA treatment and IDD + *Postn*$^{-/-}$ groups compared to the IDD + PBS group, along with increased disc height and ECM components (Fig. 8J). Histopathological score based on MRI, H&E, and Safranin O-Fast Green staining consistently indicated a reduction in histopathological score for lumbar discs following GA treatment, similar to the IDD + *Postn*$^{-/-}$ group ($P < 0.05$, Fig. 8K).

We also investigated POSTN expression levels in each group. IHC staining analyses revealed a significant increase in POSTN expression in the IDD + PBS group, which was markedly reduced following GA treatment ($P < 0.05$, Fig. 8L-M). Subsequent IF staining of IVD tissue in rats showed expression of ECM synthesis and metabolism-related molecules (Col II and MMP13) as well as pyroptosis-related molecules (NLRP3 and GSDMD-N) across groups. The results indicated that fluorescence intensity of MMP13, NLRP3, and GSDMD-N was highest in the IDD + PBS group, while Col II fluorescence intensity was lowest. Following GA treatment, fluorescence intensity of MMP13, NLRP3, and GSDMD-N decreased, whereas Col II intensity increased in the IDD + GA (10 mg/kg), IDD + GA (20 mg/kg), and IDD + *Postn*$^{-/-}$ groups compared to the IDD + PBS group ($P < 0.05$, Fig. 8N-O). In summary, findings from both in vivo and in vitro studies suggest that GA treatment significantly delays the progression of IDD in rats, potentially through the inhibition of POSTN expression, with the specific mechanism illustrated in Fig. 9.

Discussion

In our previous research, we established that POSTN expression is significantly elevated in IDD and positively correlates with Pfirrmann grading [30]. We also demonstrated that POSTN promotes aging, apoptosis, and ECM metabolism in NP cells via the activation of Wnt/β-catenin and NF-κB (P65) signaling pathways, contributing to the progression of IDD [28, 29]. To further elucidate the mechanisms by which POSTN influences IDD, we constructed NP cells overexpressing POSTN and performed transcriptome sequencing analysis. Our findings identified DEGs primarily associated with inflammatory cell apoptosis, positive regulation of interleukin-6 production, and cellular responses to interleukin-1. KEGG enrichment analysis revealed significant

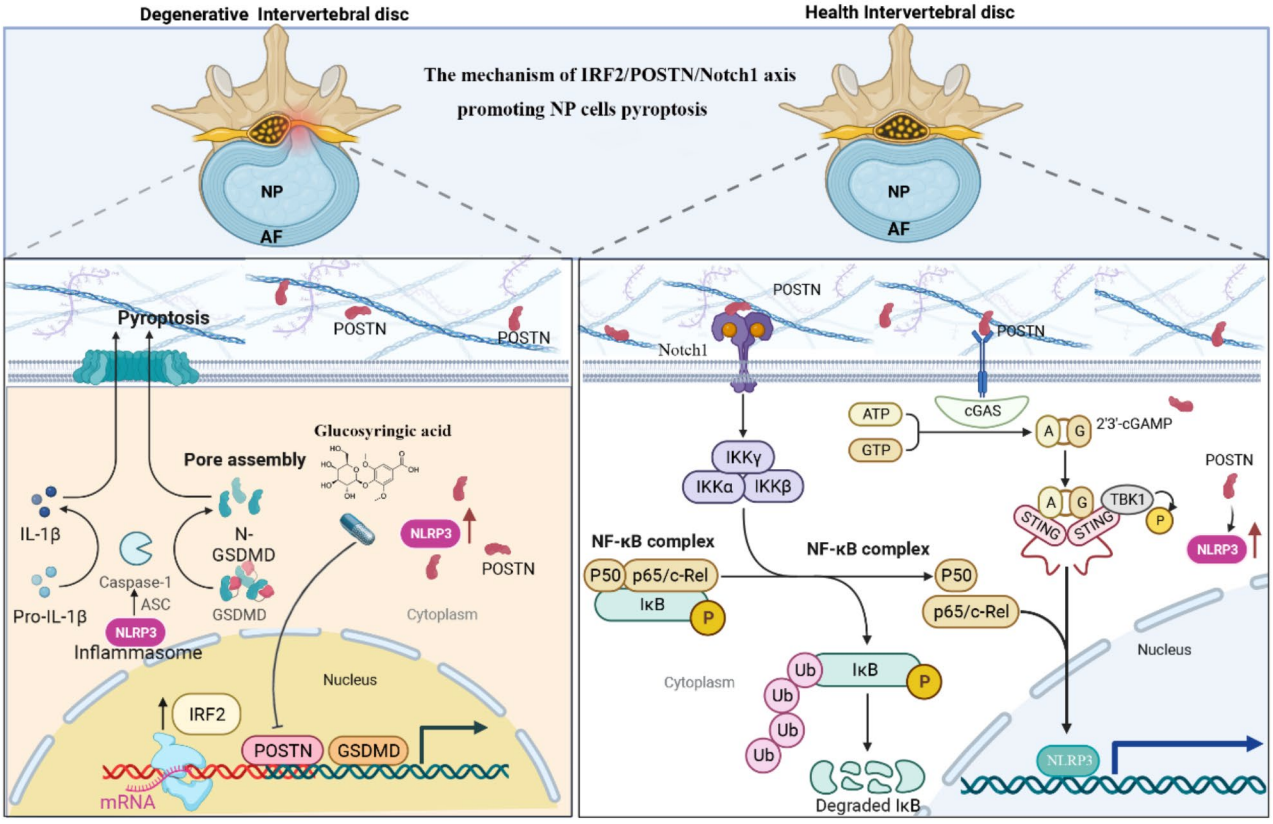

Fig. 9 Schematic diagram illustrating that IRF2/POSTN/Notch1 axis promotes NP cells pyroptosis via activating NLRP3 inflammasome in IDD

associations with the NF-κB (P65) signaling pathway, NOD-like receptor signaling pathway, and pyroptosis, suggesting that POSTN may mediate the progression of IDD through pyroptosis in NP cells.

This study is the first to demonstrate the critical role of POSTN in activating the NLRP3 inflammasome and inducing pyroptosis in NP cells. Our in vitro experiments indicate that POSTN overexpression enhances NLRP3 inflammasome activity and pyroptosis, while its knockdown effectively mitigates IL-1β-induced NLRP3 activation and pyroptosis. These findings align with previous reports by Yao et al. [32] and Bian et al. [31], which highlight the role of POSTN in promoting pyroptosis in various contexts. To validate the involvement of POSTN in IDD, we established a puncture-induced IDD model in Postn-/- rats, demonstrating that inhibiting POSTN expression significantly reduces NLRP3 inflammasome activity and pyroptosis, thereby delaying IVD degeneration. This provides new insights into POSTN's role in IDD and suggests potential molecular targets for therapeutic intervention.

In this study, we investigate the specific mechanisms by which POSTN activates the NLRP3 inflammasome, revealing that this activation occurs through the NF-κB (P65) and cGAS/STING signaling pathways. Our findings align with previous research indicating that the NF-κB (P65) pathway mediates NLRP3 expression, leading to pyroptosis in NP cells, which is a critical process in IDD [41–43]. Targeting this pathway to inhibit pyroptosis presents a promising therapeutic strategy for alleviating IDD symptoms. Several studies have demonstrated that compounds such as Notoginsenoside R1 [44], Maltol [45], and platelet-rich plasma-derived extracellular vesicles [46] can inhibit the NF-κB (P65)/NLRP3 pathway, thereby reducing pyroptosis and inflammation in endplate chondrocytes. Additionally, cGAS, functioning as an intracellular DNA sensor, can recognize both exogenous and endogenous signals, triggering downstream reactions through the STING pathway [47, 48]. The activation of the cGAS/STING pathway has been shown to exacerbate inflammatory responses in NP cells, further promoting NLRP3 activation during IDD [35]. For instance, Luo et al. [49] demonstrated that the cGAS/STING axis contributes to sepsis-induced acute kidney injury by activating the NLRP3 inflammasome. Moreover, Yang et al. [50] found that inhibiting cGAS reduced NLRP3 activation and cognitive dysfunction in mice. Similarly, Tian et al. [51] reported that epigallocatechin-3-gallate can protect NP cells from apoptosis and inflammation by inhibiting the cGAS/STING/NLRP3 signaling

pathway. Collectively, these findings underscore the significant role of the NF-κB (P65) and cGAS/STING pathway in IDD, particularly in promoting NLRP3 activation.

This study elucidates the mechanism by which POSTN activates the NF-κB (P65) pathway through its interaction with Notch1, thereby mediating the activation of the NLRP3 inflammasome in the context of IDD. Our findings highlight a novel connection between POSTN and Notch1, suggesting that the Notch1/NF-κB (P65)/NLRP3 signaling axis plays a crucial role in the inflammatory processes associated with IDD. Previous studies have established that inflammatory cytokines, such as IL-1β and TNF-α, can induce Notch signaling in NP cells, implicating Notch1 in the pathogenesis of IDD [52, 53]. Furthermore, Wei et al. [54] demonstrated that FAM83H-AS1 promotes NP cell growth and modulates ECM expression through Notch1 targeting. Additionally, BMP9 has been shown to inhibit Notch signaling, promoting ECM formation in NP cells, further underscoring the significance of Notch1 in IDD pathology [55]. These findings align with our results, indicating that Notch1 is a pivotal player in the inflammatory response within the disc microenvironment. The precursor Notch1 protein (p300) is cleaved by furin protease in the trans-Golgi network, resulting in the formation of the extracellular and cytoplasmic domains [56]. Ligand binding triggers a series of proteolytic events, ultimately leading to the release of the NICD [57]. The NICD then translocates to the nucleus, where it binds to the DNA-binding protein CBF1, thereby activating the transcription of multiple effector genes, including NF-κB (P65) [58, 59]. Our study adds to the existing literature by demonstrating the direct interaction between POSTN and Notch1, which leads to the activation of NF-κB (P65). This interaction is particularly relevant as the binding of p65 with the domain of NICD1 is essential for the NF-κB signaling pathway activation triggered by inflammatory stimuli. This crosstalk between Notch1 and NF-κB (P65) has implications beyond IDD; for instance, it has been observed in glioblastoma cells, where Notch1 influences cell proliferation and apoptosis [60]. Moreover, recent evidence suggests that Notch1 can activate NF-κB (P65) via TLR4 in macrophages [61], highlighting the broader relevance of this signaling interplay in inflammatory contexts. The relationship between Notch1 and NLRP3 inflammasome activity is also well-documented. Studies indicate that Notch1 signaling can regulate NLRP3-driven inflammatory responses in various conditions, including liver injury and endometriosis [37, 62].

However, some studies present an opposing viewpoint. Liao et al. [63] conducted an in-depth investigation of the therapeutic mechanism of small extracellular vesicles and found that the vasorin protein enriched in these vesicles promoted the proliferation and ECM anabolism of NP cells through the Notch1 signal pathway. The discrepancies in these research findings may be attributed to the specific roles played by the frequency and duration of Notch signal activation [64]. Some studies have shown that continuous activation of Notch1 signal in IVDs after birth in mice severely damages growth plate and endplate cartilage tissue [64]. In articular cartilage, continuous Notch signal transmission leads to early and progressive osteoarthritis-like pathology; however, under normal physiological conditions, brief Notch signal activation can enhance the synthesis of cartilage matrix and promote joint maintenance [65]. Therefore, specific regulation of Notch signal may be considered in the treatment of IDD.

The interferon regulatory factors (IRFs) family, consisting of nine members (IRF1-9), plays a crucial role as nuclear transcription factors in mammals, influencing a wide array of biological processes such as apoptosis, cell differentiation, proliferation, immune responses, and tumorigenesis [66–68]. Among these factors, IRF2 has emerged as a significant regulator of cell death pathways, particularly through its transcriptional regulation of genes including Toll-like receptor 3, Bcl-11a, and GSDMD [40, 69, 70]. Our findings reveal that IRF2 binds to the promoter region of the POSTN gene in NP cells, thereby enhancing its transcription. This activation subsequently induces the NLRP3 inflammasome and facilitates pyroptosis. Notably, this study is the first to characterize the expression of IRF2 in the context of IDD, demonstrating an upregulation of IRF2 in NP cells. Functional experiments indicate that the knockdown of IRF2 significantly mitigates IL-1β-induced NLRP3 activation and pyroptosis, while overexpression of IRF2 exacerbates these effects. Interestingly, the partial reversal of this exacerbation upon reducing POSTN expression suggests a complex regulatory feedback loop that warrants further investigation. Furthermore, the role of IRF2 in regulating GSDMD expression is particularly noteworthy. Our results are consistent with previous studies that have identified IRF2 as a transcriptional activator of GSDMD, thereby establishing a direct link to the pyroptotic pathway [71]. Supporting our observations, the findings of Kayagaki et al. [40]. reinforce the notion that IRF2 is integral to the transcriptional regulation of key components involved in pyroptosis. In summary, our study provides novel insights into the role of IRF2 in IDD, demonstrating its direct involvement in the regulation of the POSTN gene and the subsequent activation of the NLRP3 inflammasome.

IDD continues to pose a significant clinical challenge, with current treatments primarily focusing on symptomatic relief through pharmacological interventions and surgical options. However, these approaches fail to address the underlying degenerative processes,

underscoring the urgent need for innovative therapeutic strategies aimed at reversing or slowing the progression of IDD [72, 73]. Previous research has demonstrated that targeting key genes in the apoptotic pathway can effectively suppress apoptosis in IVD cells, thereby slowing degeneration [74]. By concentrating on the molecular players involved in these pathways, we can develop strategies that may alleviate degenerative processes at a genetic level. In this context, POSTN emerges as a critical factor in the pathological processes associated with IDD. The potential development of POSTN inhibitors could represent a significant advancement in the treatment of this condition. Our study identifies a plant-derived compound, GA, which directly binds to POSTN and inhibits its expression. Experiments conducted in both cellular and animal models indicate that GA effectively ameliorates the pathological changes associated with IDD by downregulating POSTN expression. This finding opens new avenues for therapeutic interventions targeting POSTN in IDD.

However, there are also some limitations in this study. First, the animal models currently used cannot fully simulate the pathological characteristics of human IDD. Second, when constructing the puncture-induced IDD model, human factors may have a certain impact on the experimental results. Although various animal models have been developed for the study of IDD, no model has been able to fully replicate the biomechanical environment of human IDD to date. In addition, although our research results suggest that regulating the expression of POSTN may be a potential strategy for treating IDD, it must be recognized that translating the findings of basic research into clinical applications is a complex and challenging process. This not only requires further in-depth exploration of mechanisms but also involves extensive preclinical and clinical research.

Conclusions

This study elucidates the mechanistic role of the IRF2/POSTN/Notch1 signaling axis in the pathogenesis of IDD, highlighting its capacity to trigger the NLRP3 inflammasome. While our findings suggest a potential link to pyroptosis in NP cells, we acknowledge that further investigation is needed to definitively establish this relationship and to rule out other types of cell death that may also be involved. The translational significance of our findings is underscored by the identification of the phytochemical GA as a potential therapeutic agent, with its demonstrated ability to suppress POSTN expression, thereby offering a novel avenue for IDD management and treatment. Future studies should focus on clarifying the specific mechanisms of cell death involved in this context to strengthen the conclusions drawn from our research.

Materials and methods

Collection of human NP specimens

Human NP samples were procured from individuals who were undergoing spinal surgical procedures. The selection of these individuals was predicated on conditions such as spinal trauma, idiopathic scoliosis, or disc herniation. Exclusion criteria included spinal infections, immunosuppressive conditions, hypertension, and diabetes. A total of 34 NP samples were collected, encompassing 14 male and 20 female participants, with ages ranging from 16 to 72 years. The extent of disc degeneration was evaluated utilizing the Pfirrmann grading system. We categorized the samples into two groups based on the degree of degeneration: a mild degeneration group, characterized by Pfirrmann grades I-II, comprising 17 samples from individuals with idiopathic scoliosis and vertebral fractures; and a severe degeneration group, denoted by Pfirrmann grades IV-V, also consisting of 17 samples sourced from various disc herniation segments. Informed consent was obtained from all patients involved in this study. The experimental designs and protocols involving human samples were approved by the Medical Ethics Committee of Lanzhou University Second Hospital, Gansu, China (Approval No: 2024 A-258). Supplementary Table 1 provides a detailed compilation of the pertinent data for each participant.

Culturing and treatment of NP cells

The immortalized human NP cell line (0028a) was sourced from Yaji Bio-technology Company (accessible via their online platform at http://www.yajimall.com/). These cells were nurtured in a DMEM/F12 medium provided by Gibco, enriched with 15% fetal bovine serum (also from Gibco) and a mixture of 1% streptomycin and penicillin antibiotics. The cell cultures were maintained in an incubation environment at 37 °C with a 5% CO^2 atmosphere. Once the cells reached full confluence, they were subcultured using 0.25% Trypsin-EDTA solution (Gibco) and then replated into 10-cm diameter culture dishes at optimal densities. Additionally, human embryonic kidney (HEK) 293 T cells were procured from Yaji Bio-technology Company located in Shanghai, China. These cells were cultivated in DMEM medium supplemented with 10% foetal bovine serum (FBS) and 1% penicillin-streptomycin mixture, under incubation conditions of 5% CO^2 at 37 °C. To elicit the pyroptosis phenotype in NP cells, IL-1β was introduced into the culture system. The cytotoxic effects of GA were evaluated by incorporating varying concentrations of GA (ranging from 5 to 200 μM, sourced from HY-N3953, MCE) into the culture medium. The cell viability was subsequently measured using a Cell Counting Kit-8 assay. Consistent with the in vitro experimental protocol, all treatments were administered with an equivalent volume of their respective

solvents: PBS for IL-1β and dimethyl sulfoxide (DMSO) for GA, CU-T12-9, and BAY. The final concentration of DMSO in the culture medium was diluted to a ratio of 1:1000.

Western blotting

Total proteins were extracted from human disc specimens and NP cells using RIPA buffer (Beyotime, China), and the protein concentration was measured by the bicinchoninic acid (BCA) assay (Beyotime, China). Subsequently, proteins were separated by sodium dodecyl sulfate-polyacrylamide gel electrophoresis (SDS-PAGE). Following blocking with 3% bovine serum albumin, the membranes were incubated with primary antibodies. Subsequently, the membranes were incubated with secondary antibodies. Finally, the proteins on the membranes were detected using enhanced chemiluminescence detection reagents (Invitrogen, CA). The PVDF membrane were purchased from Millipore (MA, USA). An informative list of the antibodies was shown in Supplementary Table 2.

Reverse transcription quantitative polymerase chain reaction (RT-qPCR) and gel electrophoresis

RT-qPCR and gel electrophoresis PCR were employed to assess the expression of relevant genes in both cell models and POSTN knockout rats. To evaluate gene expression in the cell models, total RNA was extracted from the cells using RNAiso Plus (Takara, Japan). The extracted mRNA was then reverse transcribed into complementary DNA (cDNA) using PrimeScript RT Master Mix (Takara). Subsequently, quantitative real-time PCR was performed using SYBR Premix Ex Taq II (Takara) and the ABI 7900HT fast real-time PCR system (Applied Biosystems, Waltham, MA), with specific primers designed for the genes of interest. The relative mRNA expression levels were calculated using the $2^{-\Delta\Delta Ct}$ method to assess gene expression changes in the cell models. Additionally, to investigate the expression of the POSTN gene in *Postn*$^{-/-}$ rats, we conducted PCR reactions followed by gel electrophoresis analysis. After the PCR reactions, the products were mixed with DNA loading buffer and loaded onto an agarose gel for electrophoresis. Upon completion of the electrophoresis, the gel was visualized under UV light using a DNA dye to confirm the expression of the POSTN gene in the *Postn*$^{-/-}$ rats.

Immunohistochemistry (IHC) stain

To conduct further analysis, sections from both human and rat discs were collected. After antigen retrieval and blocking with 5% normal goat serum, the slides were subjected to incubation with primary antibodies and secondary antibodies. Subsequently, the sections were treated with DAB solution (Gene-Tech, Shanghai, China) for development and counterstained with hematoxylin. Histological fields were randomly selected in each section and captured at 200× magnification using an Olympus BX63 microscope (Olympus, Japan). The histological fields were observed at a magnification of 200× using the same microscope. The percentage of positive cells was calculated using Image J software (National Ins titutes of Health). The information of antibodies was shown in Supplementary Table 2.

Generation of knockdown cell

Specific protocols for creating knockdown cells are available in a prior publication. Transfected cells were chosen using puromycin at specified doses (1–5 μg/mL), expanded through multiple passages, and cryopreserved for future cellular investigations.

RNA-seq data analysis

The analysis of RNA-seq data involved sending POSTN overexpression NP cells and control NP cells for high-throughput transcriptome sequencing on the Illumina HiSeq platform at Qinglian Biotechnology (Beijing) Co., Ltd. DESeq2 software was utilized to detect differentially expressed genes (DEGs) between the experimental groups, with $|\log2FC| \geq 1$ and $P < 0.05$ set as the selection criteria. Subsequently, the identified DEGs underwent enrichment analysis using the Kyoto Encyclopedia of Genes and Genomes (KEGG) and Gene Ontology (GO) databases.

GO: Gene Ontology.

Bioinformatic analysis

The construction of a protein-protein interaction (PPI) network was carried out through analysis of the String database. Gene expression correlation analysis was conducted using the GEPIA database. By utilizing the GeneCards, CTD, and DisGeNET databases, a total of 1241 genes related to pyroptosis were identified. Predictions of POSTN transcription factors were acquired from the HumanTFDB, hTFtarget databases, and JASPAR database, leading to the discovery of 321 potential transcription factors capable of regulating POSTN. Supplementary Table 3 contains the links to the databases referenced.

Chromatin immunoprecipitation (ChIP) assay

After necessary processing, cells were collected for ChIP experiment to demonstrate the DNA sequence of the POSTN promoter bound by IRF2. According to the manufacturer's instructions, the experiment was conducted using the ChIP assay kit (Abcam, Ab185913). Cells were cross-linked with 1% formaldehyde for 10 min and the reaction was stopped with 125 mM glycine. After chromatin isolation, DNA fragments associated with the binding protein were collected. The lysate samples from

each chromatin solution were immunoprecipitated overnight at 4 °C with IRF2 antibody or pre-immune IgG, isolating the complex containing the target protein and its bound DNA. Subsequently, DNA was released by reverse cross-linking and proteins were digested. Next, Agarose Gel Electrophoresis was conducted to detect the precipitated genomic DNA using primers specific to the IRF2 binding site. The non-precipitated genomic DNA served as an input control for amplification.

Luciferase reporter assay

The human IRF2 gene was cloned and inserted into the pcDNA3.1 plasmid (pCDNA3.1-IRF2). Subsequently, the promoter sequences of the human POSTN and GSDMD genes were individually inserted into the pGL3-Basic plasmid, resulting in the recombinant plasmids labeled as pGL3-POSTN and pGL3-GSDMD. These recombinant plasmids, in conjunction with the pRL-TK plasmid containing the Renilla luciferase reporter gene sequence, were co-transfected into 293T and NP cells. Upon reaching optimal cell density, the cells were lysed and the lysate was collected. Subsequently, the luciferase detection reagent and Renilla luciferase detection reagent were added to the detection instrument for fluorescence intensity measurement. Ultimately, the ratio of the relative light units (RLU-1) of the firefly luciferase to the relative light units (RLU-2) of the Renilla luciferase, i.e., RLU-1/RLU-2, was utilized as the internal reference for the activation level of the target gene in each sample tested. This standardized approach ensures the precision and comparability of the experimental outcomes.

Immunofluorescence (IF) staining

NP cells were seeded into flat-bottom 24-well plates at a density of 5×10^3 cells per well. Subsequently, they were incubated with 4% paraformaldehyde, permeabilized with 0.5% Triton-X 100 in phosphate-buffered saline (PBS) for 10 min, and blocked with PBS containing 1% BSA. Tissue sections were blocked for 1 h using 10% BSA after baking, dewaxing, hydration, and antigen retrieval steps. The sections and cells were then incubated overnight with a primary antibody. The next day, after washing, the cells and tissue sections were treated with a 1:300 dilution of Alexa Fluor-488 or -594 conjugated anti-rabbit or anti-mouse secondary antibody (Immunoway, USA) for 1 h at room temperature before being imaged using a laser scanning confocal microscope (Olympus, Tokyo, Japan).

Hematoxylin-eosin (H&E) and Safranine-O/Fast green staining

The tissue paraffin blocks were cut into 4 μm sections for histological analysis of both human samples and rat discs, utilizing H&E and Safranine-O/Fast green staining. Additionally, all rats were euthanized 8 weeks after surgery, and disc tissue Sect. (5 μm) were prepared and processed as previously described for H&E and Safranin-O/Fast Green staining to assess the extent of IDD. Images were captured with a light microscope.

Magnetic resonance imaging (MRI)

Eight weeks post-surgery, MRI scans of the coccyx were conducted. During the examinations, all rats were anesthetized and their tails were kept straight. A total of 54 rats, six from each group, underwent sagittal and horizontal T2-weighted imaging using a 3.0-T clinical magnet (Philips Intera Achieva 3.0MR). The T2-weighted imaging parameters included a fast-spin echo sequence with a repetition time of 5400 ms and an echo time of 920 ms; a matrix of 320 (h) × 256 (v); a field of view of 260°; and four excitations. The section thickness was set at 2 mm with no gap. All MR images were analyzed in a blinded manner according to the IDD classification system by Pfirrmann et al.

Co-immunoprecipitation (Co-IP) assay

Cells were harvested and lysed using RIPA lysis buffer (Beyotime, Shanghai, China) supplemented with a protease inhibitor cocktail (Beyotime, Shanghai, China). Whole-cell lysates (2 mg) were pre-cleared with 30 μL of protein G beads (Abmart, Shanghai, China). Subsequently, 2 μg of either isotype-matched IgG control or the specified antibodies were added and incubated for 2 h on a rocking platform. The immunoprecipitates were collected via centrifugation and then subjected to SDS-PAGE for resolution. A detailed list of the antibodies used is provided in Supplementary Table 2.

Senescence-associated β-galactosidase (SA-β-gal) staining

The extent of cellular senescence was assessed using the SA-β-gal staining kit (Beyotime, Shanghai, China) following the manufacturer's instructions. Senescent NP cells, which exhibited increased SA-β-gal activity, were stained blue.

Construction of a POSTN gene knockout rat model

To create a rat model with a POSTN gene knockout, we used CRISPR/Cas9 gene-editing technology. First, we identified the precise location of the POSTN gene using genomic databases and designed a specific guide RNA (sgRNA) to target this gene. The sgRNA facilitated DNA double-strand breaks mediated by the Cas9 protein, achieving the knockout. After obtaining the sgRNA sequence, we synthesized it and co-transfected it with the Cas9 protein complex into rat zygotes under controlled conditions to ensure high gene-editing efficiency. The microinjected zygotes were then cultured in a specific medium for further development. We used embryo implantation techniques to transfer the edited embryos

into surrogate mothers. This involved careful surgical procedures to implant the embryos into the uteri of the surrogate mothers, resulting in offspring with the POSTN gene knocked out. After birth, we used molecular biology techniques such as PCR and sequence analysis to genotype the offspring and select those with a successful POSTN gene knockout. The entire process adhered strictly to the animal use and care guidelines of the affiliated institution, ensuring ethical and scientific integrity.

Establishment of IDD rat model

Before performing aseptic surgery to induce IDD in rats, we administered anesthesia via an injection of pentobarbital sodium (45 mg/kg). Rats weighing 200–250 g were placed in a prone position, and a midline longitudinal incision was made on the tail. The left or right facet joint between the seven and eight caudal vertebrae was removed to expose the Co7/8 disc. IDD was induced by inserting a 30-gauge needle parallel to the endplates, penetrating 3.0 mm into the disc and leaving it in place for 30 s. The control group received no intervention. Muscle closure was done with 3 – 0 silk sutures, and the skin was sutured with 4 – 0 nylon sutures. Four weeks post-operation, MRI, H&E staining and Safranin-O/Fast Green staining were performed on caudal vertebrae of rats.

Molecular docking

The POSTN structure (5YJH) was obtained from the Protein Data Bank (https://www.rcsb.org) based on its UniProt ID, while the structure of GA was retrieved from the PubChem database (https://pubchem.ncbi.nlm.nih.gov/). The receptor molecules of the target protein underwent hydrogenation and charge calculations utilizing AutoDockTools (version 4.2.6), with the active site defined as the binding pocket of the protein's native ligand. Molecular docking analyses were performed using Vina 1.5.6. Finally, the three-dimensional representation of the docking outcomes was visualized using PyMOL software.

Drug screening

To investigate the effects of 390 natural products on POSTN promoter activity, we developed a small molecule library and performed assays utilizing a luciferase reporter gene. Specifically, the full-length promoter region of the *POSTN* gene, extending from −2995 bp to the transcription start site, was cloned into the pGL3 luciferase vector (Beijing Tsingke Biotech Co., Ltd.). The luciferase reporter gene plasmid was then transfected into NP cells and cultured for 48 h. After this incubation period, various compounds (5 μM) were introduced under IL-1β treatment conditions for an additional 24 h. Finally, the relative activity of firefly luciferase was assessed using a dual luciferase reporter assay kit (Beijing Tsingke Biotech Co., Ltd.).

Annulus needle puncture and drug treatment

We utilized 30 adult male SD rats (200–250 g) obtained from the Gansu Science Animal Center in China. The rats were randomly divided into five groups: sham surgery, IDD + PBS, IDD + GA (10 mg/kg), IDD + GA (20 mg/kg), and IDD + *Postn*$^{-/-}$, with 6 rats in each group. Rats in the IDD + GA groups received intraperitoneal injections of 10 or 20 mg/kg GA every other day starting from the day of surgery. The IDD + PBS group received daily intraperitoneal injections of an equal volume of PBS. The IDD + *Postn*$^{-/-}$ group served as the positive control. All rats were housed in pathogen-free cages with ad libitum access to autoclaved food and reverse osmosis water, in rooms with controlled temperature and humidity under a 12 h light/dark cycle. Six weeks post-surgery, rats underwent MRI to assess signal changes and the severity of IDD using the Pfirrmann classification. Euthanasia was performed by anesthesia with 5% isoflurane, confirmed by a tail pinch, followed by cervical dislocation at the atlanto-occipital joint. IVD tissues were harvested for fixation, dehydration, decalcification, embedding, and sectioning for further experiments. All procedures were reviewed and approved by the Ethics Committee of the Second Hospital of Lanzhou University (Approval No: D2024-303). The study adhered to the ethical standards outlined in the Laboratory Animal Care and Use Guide (NIH, 2011), the Basel Declaration, and the Helsinki Declaration of 1964, ensuring scientific and ethical integrity.

Statistical analysis

The cellular and molecular experiments in this study were repeated independently at least three times, while the animal assays were repeated with at least six mice. The data obtained from these replications were averaged and presented as the mean value ± standard deviation (SD). Statistical analysis was carried out using GraphPad Prism 5.0 (GraphPad Software, Inc., San Diego, CA, USA). Differences between two groups were determined using an unpaired t-test, and the statistical significance of correlations was evaluated through Pearson's correlation coefficient analysis. Analysis of variance (ANOVA) was conducted for comparing multiple groups, with statistical significance set at $P < 0.05$.

Abbreviations

AF	Annulus fibrosus
ChIP	Chromatin immunoprecipitation
Co-IP	Co-immunoprecipitation
DEGs	Differentially expressed genes
ECM	Extracellular matrix
GA	Glucosyringic acid
GO	Gene Ontology
GSDMD	Gasdermin D

IDD	Intervertebral disc degeneration
IF	Immunofluorescence
IHC	Immunohistochemistry
IL-1β	Interleukin 1 beta
IRF2	Interferon regulatory factor 2
IVD	Intervertebral disc
KEGG	Kyoto encyclopedia of genes and genomes
NLRP3	NOD-Like receptor protein 3
NICD	Notch intracellular domain
NP	Nucleus pulposus
POSTN	Periostin
WT	Wild type

Supplementary Information

The online version contains supplementary material available at https://doi.org/10.1186/s12974-025-03335-4.

Supplementary Material 1

Supplementary Material 2

Author contributions

Daxue Zhu, Zhaoheng Wang, and Shijie Chen contributed equally to this article. Daxue Zhu put on the reference collection, reference analysis, manuscript writing, and topic conception, Zhaoheng Wang, Shijie Chen, and Yanhu Li contributed to reference analysis and helped revise the manuscript. Xuewen Kang, the corresponding author, contributed to revising the manuscript and figures and decided to submit them for publication.

Funding

This work was supported by National Natural Science Foundation of China (82272536), Natural Science Foundation of Gansu Province (23JRRA1012), "Innovation Star" of the Second Hospital of Lanzhou University(2025CXZX-117).

Data availability

No datasets were generated or analysed during the current study.

Declarations

Ethics approval and consent to participate

All experimental designs and protocols involving animals and human samples were approved by the Animal Ethics Committee and Medical Ethics Committee of Lanzhou University Second Hospital, Gansu, People's Republic of China (approval D2023-303 and 2023 A-258) and complied with the recommendations of the academy's animal research guidelines.

Consent for publication

All authors gave their consent for publication.

Competing interests

The authors declare no competing interests.

Received: 20 August 2024 / Accepted: 6 January 2025
Published online: 22 January 2025

References

1. Moore RJ. The vertebral endplate: disc degeneration, disc regeneration. Eur Spine Journal: Official Publication Eur Spine Soc Eur Spinal Deformity Soc Eur Sect Cerv Spine Res Soc. 2006;15(Suppl 3):S333–7.
2. Collaborators, GDallaP. Global, regional, and national incidence, prevalence, and years lived with disability for 328 diseases and injuries for 195 countries, 1990–2016: a systematic analysis for the global burden of Disease Study 2016. Lancet (London England). 2017;390:1211–59.
3. Roberts S, Menage J, Duance V, Wotton S, Ayad S. 1991 Volvo Award in basic sciences. Collagen types around the cells of the intervertebral disc and cartilage end plate: an immunolocalization study. Spine (Phila Pa 1976). 1991;16:1030–8.
4. Adams MA, Dolan P, McNally DS. The internal mechanical functioning of intervertebral discs and articular cartilage, and its relevance to matrix biology. Matrix Biology: J Int Soc Matrix Biology. 2009;28:384–9.
5. Vasudevan SO, Behl B, Rathinam VA. Pyroptosis-induced inflammation and tissue damage. Semin Immunol. 2023;69:101781.
6. Yu P, Zhang X, Liu N, Tang L, Peng C, Chen X. Pyroptosis: mechanisms and diseases. Signal Transduct Target Ther. 2021;6:128.
7. Zhao K, An R, Xiang Q, Li G, Wang K, Song Y, Liao Z, Li S, Hua W, Feng X, et al. Acid-sensing ion channels regulate nucleus pulposus cell inflammation and pyroptosis via the NLRP3 inflammasome in intervertebral disc degeneration. Cell Prolif. 2021;54:e12941.
8. Ma Z, Tang P, Dong W, Lu Y, Tan B, Zhou N, Hao J, Shen J, Hu Z. SIRT1 alleviates IL-1β induced nucleus pulposus cells pyroptosis via mitophagy in intervertebral disc degeneration. Int Immunopharmacol. 2022;107:108671.
9. Wu S, Liu S, Huang R, Zhou Y, Zou Y, Yang W, Zhang J. Adiponectin inhibits LPS-induced nucleus pulposus cell pyroptosis through the miR-135a-5p/TXNIP signaling pathway. Aging. 2023;15:13680–92.
10. Vergroesen PPA, Kingma I, Emanuel KS, Hoogendoorn RJW, Welting TJ, van Royen BJ, van Dieën JH, Smit TH. Mechanics and biology in intervertebral disc degeneration: a vicious circle. Osteoarthr Cartil. 2015;23:1057–70.
11. Chen S, Fu P, Wu H, Pei M. Meniscus, articular cartilage and nucleus pulposus: a comparative review of cartilage-like tissues in anatomy, development and function. Cell Tissue Res. 2017;370:53–70.
12. Luo J, Yang Y, Wang X, Chang X, Fu S. Role of Pyroptosis in intervertebral disc degeneration and its therapeutic implications. Biomolecules. 2022;12.
13. Zhou D, Mei Y, Song C, Cheng K, Cai W, Guo D, Gao S, Lv J, Liu T, Zhou Y et al. Exploration of the mode of death and potential death mechanisms of nucleus pulposus cells. Eur J Clin Invest. 2024:54(9):e14226.
14. Takeshita S, Kikuno R, Tezuka K, Amann E. Osteoblast-specific factor 2: cloning of a putative bone adhesion protein with homology with the insect protein fasciclin I. Biochem J. 1993;294(Pt 1):271–8.
15. Kudo A. Naming, History, Future. Adv Exp Med Biol. 2019;1132:3–4.
16. Liu J, Zhang J, Xu F, Lin Z, Li Z, Liu H. Structural characterizations of human periostin dimerization and cysteinylation. FEBS Lett. 2018;592:1789–803.
17. Lin JH, Lin IP, Ohyama Y, Mochida H, Kudo A, Kaku M, Mochida Y. FAM20C directly binds to and phosphorylates Periostin. Sci Rep. 2020;10:17155.
18. Solanki B, Prakash A, Rehan HS, Gupta LK. Effect of inhaled corticosteroids on serum periostin levels in adult patients with mild-moderate asthma. Allergy Asthma Proc. 2019;40:32–4.
19. Burgess JK, Jonker MR, Berg M, Ten Hacken NTH, Meyer KB, van den Berge M, Nawijn MC. Heijink IH: Periostin: contributor to abnormal airway epithelial function in asthma? Eur Respir J. 2020;17;57(2):2001286.
20. Fan B, Liu X, Chen X, Xu W, Zhao H, Yang C, Zhang S. Periostin mediates condylar resorption via the NF-κB-ADAMTS5 pathway. Inflammation. 2020;43:455–65.
21. Attur M, Duan X, Cai L, Han T, Zhang W, Tycksen ED, Samuels J, Brophy RH, Abramson SB, Rai MF. Periostin loss-of-function protects mice from post-traumatic and age-related osteoarthritis. Arthritis Res Ther. 2021;23:104.
22. Rachner TD, Gobel A, Hoffmann O, Erdmann K, Kasimir-Bauer S, Breining D, Kimmig R, Hofbauer LC, Bittner AK. High serum levels of periostin are associated with a poor survival in breast cancer. Breast Cancer Res Treat. 2020;180:515–24.
23. Yang T, Deng Z, Pan Z, Qian Y, Yao W, Wang J. Prognostic value of periostin in multiple solid cancers: a systematic review with meta-analysis. J Cell Physiol. 2020;235:2800–8.
24. Rai MF, Tycksen ED, Sandell LJ, Brophy RH. Advantages of RNA-seq compared to RNA microarrays for transcriptome profiling of anterior cruciate ligament tears. J Orthop Res. 2018;36:484–97.
25. Sanchez C, Mazzucchelli G, Lambert C, Comblain F, DePauw E, Henrotin Y. Comparison of secretome from osteoblasts derived from sclerotic versus non-sclerotic subchondral bone in OA: a pilot study. PLoS ONE. 2018;13:e0194591.
26. Tajika Y, Moue T, Ishikawa S, Asano K, Okumo T, Takagi H, Hisamitsu T. Influence of Periostin on synoviocytes in knee osteoarthritis. Vivo. 2017;31:69–77.
27. Han T, Mignatti P, Abramson SB, Attur M. Periostin interaction with discoidin domain receptor-1 (DDR1) promotes cartilage degeneration. PLoS ONE. 2020;15:e0231501.
28. Zhu D, Wang Z, Zhang G, Ma C, Qiu X, Wang Y, Liu M, Guo X, Chen H, Deng Q, Kang X. Periostin promotes nucleus pulposus cells apoptosis by activating

the Wnt/β-catenin signaling pathway. FASEB Journal: Official Publication Federation Am Soc Experimental Biology. 2022;36:e22369.
29. Wu J, Chen Y, Liao Z, Liu H, Zhang S, Zhong D, Qiu X, Chen T, Su D, Ke X et al. Self-amplifying Loop of NF-kappaB and Periostin initiated by PIEZO1 accelerates Mechano-induced senescence of Nucleus Pulposus cells and intervertebral disc degeneration. Mol Ther. 2022;5;30(10):3241-3256.
30. Zhu D, Chen S, Sheng P, Wang Z, Li Y, Kang X. POSTN promotes nucleus pulposus cell senescence and extracellular matrix metabolism via activing Wnt/β-catenin and NF-κB signal pathway in intervertebral disc degeneration. Cell Signal. 2024;121:111277.
31. Bian X, Su X, Wang Y, Zhao G, Zhang B, Li D. Periostin contributes to renal and cardiac dysfunction in rats with chronic kidney disease: reduction of PPARα. Biochimie. 2019;160:172–82.
32. Yao L, Song J, Meng XW, Ge JY, Du BX, Yu J, Ji FH. Periostin aggravates NLRP3 inflammasome-mediated pyroptosis in myocardial ischemia-reperfusion injury. Mol Cell Probes. 2020;53:101596.
33. Li N, Zhou H, Wu H, Wu Q, Duan M, Deng W, Tang Q. STING-IRF3 contributes to lipopolysaccharide-induced cardiac dysfunction, inflammation, apoptosis and pyroptosis by activating NLRP3. Redox Biol. 2019;24:101215.
34. Zhang G-Z, Liu M-Q, Chen H-W, Wu Z-L, Gao Y-C, Ma Z-J, He X-G. Kang X-W: NF-κB signalling pathways in nucleus pulposus cell function and intervertebral disc degeneration. Cell Prolif. 2021;54:e13057.
35. Zhang W, Li G, Luo R, Lei J, Song Y, Wang B, Ma L, Liao Z, Ke W, Liu H, et al. Cytosolic escape of mitochondrial DNA triggers cGAS-STING-NLRP3 axis-dependent nucleus pulposus cell pyroptosis. Exp Mol Med. 2022;54:129–42.
36. Wang Z, Zhu D, Yang F, Chen H, Kang J, Liu W, Lin A, Kang X. POSTN knockdown suppresses IL-1β-induced inflammation and apoptosis of nucleus pulposus cells via inhibiting the NF-κB pathway and alleviates intervertebral disc degeneration. J Cell Commun Signal. 2024;18:e12030.
37. Zhang M, Shi Z, Peng X, Cai D, Peng R, Lin Y, Dai L, Li J, Chen Y, Xiao J, et al. NLRP3 inflammasome-mediated pyroptosis induce Notch signal activation in endometriosis angiogenesis. Mol Cell Endocrinol. 2023;574:111952.
38. Wu D, Jiang T, Zhang S, Huang M, Zhu Y, Chen L, Zheng Y, Zhang D, Yu H, Yao G, Sun L. Blockade of Notch1 signaling alleviated Podocyte Injury in Lupus Nephritis Via Inhibition of NLRP3 inflammasome activation. Inflammation. 2024;47:649–63.
39. Oswald F, Liptay S, Adler G, Schmid RM. NF-kappaB2 is a putative target gene of activated Notch-1 via RBP-Jkappa. Mol Cell Biol. 1998;18:2077–88.
40. Nobuhiko Kayagaki1 BLL, Irma B, Stowe OS, Kornfeld, Karen O'Rourke,Kathleen M Mirrashidi1, Benjamin Haley, Colin Watanabe, Merone Roose-Girma, Zora Modrusan, Sarah Kummerfeld3, Rohit Reja, Zhang Y, Cho V, Daniel Andrews T, Lucy X, Morris CC, Goodnow EM, Bertram, Vishva M. Dixit: IRF2 transcriptionally induces GSDMD expressionfor pyroptosis. Sci Signal. 2019;21:eaax4917.
41. Guo D, Cheng K, Song C, Liu F, Cai W, Chen J, Mei Y, Zhou D, Gao S, Wang G, Liu Z. Mechanisms of inhibition of nucleus pulposus cells pyroptosis through SDF1/CXCR4-NFkB-NLRP3 axis in the treatment of intervertebral disc degeneration by Duhuo Jisheng Decoction. Int Immunopharmacol. 2023;124:110844.
42. Sun Y, Leng P, Song M, Li D, Guo P, Xu X, Gao H, Li Z, Li C, Zhang H. Piezo1 activates the NLRP3 inflammasome in nucleus pulposus cell-mediated by ca(2+)/NF-κB pathway. Int Immunopharmacol. 2020;85:106681.
43. Lu P, Zheng H, Meng H, Liu C, Duan L, Zhang J, Zhang Z, Gao J, Zhang Y, Sun T. Mitochondrial DNA induces nucleus pulposus cell pyroptosis via the TLR9-NF-κB-NLRP3 axis. J Transl Med. 2023;21:389.
44. Tang K, Su W, Huang C, Wu Y, Wu X, Lu H. Notoginsenoside R1 suppresses inflammatory response and the pyroptosis of nucleus pulposus cells via inactivating NF-κB/NLRP3 pathways. Int Immunopharmacol. 2021;101:107866.
45. Gong Y, Qiu J, Jiang T, Li Z, Zhang W, Zheng X, He Z, Chen W, Wang Z, Feng X, et al. Maltol ameliorates intervertebral disc degeneration through inhibiting PI3K/AKT/NF-κB pathway and regulating NLRP3 inflammasome-mediated pyroptosis. Inflammopharmacology. 2023;31:369–84.
46. Tao X, Xue F, Xu J, Wang W. Platelet-rich plasma-derived extracellular vesicles inhibit NF-κB/NLRP3 pathway-mediated pyroptosis in intervertebral disc degeneration via the MALAT1/microRNA-217/SIRT1 axis. Cell Signal. 2024;117:111106.
47. Gaidt MM, Ebert TS, Chauhan D, Ramshorn K, Pinci F, Zuber S, O'Duill F, Schmid-Burgk JL, Hoss F, Buhmann R, et al. The DNA inflammasome in human myeloid cells is initiated by a STING-Cell death program Upstream of NLRP3. Cell. 2017;171:1110–e11241118.
48. Liu J, Zhang X, Wang H. The cGAS-STING-mediated NLRP3 inflammasome is involved in the neurotoxicity induced by manganese exposure. Biomed Pharmacother. 2022;154:113680.
49. Luo X, Zhao Y, Luo Y, Lai J, Ji J, Huang J, Chen Y, Liu Z, Liu J. Cytosolic mtDNA-cGAS-STING axis contributes to sepsis-induced acute kidney injury via activating the NLRP3 inflammasome. Clin Exp Nephrol. 2024;28:375–90.
50. Yang NS, Zhong WJ, Sha HX, Zhang CY, Jin L, Duan JX, Xiong JB, You ZJ, Zhou Y, Guan CX. mtDNA-cGAS-STING axis-dependent NLRP3 inflammasome activation contributes to postoperative cognitive dysfunction induced by sevoflurane in mice. Int J Biol Sci. 2024;20:1927–46.
51. Tian Y, Bao Z, Ji Y, Mei X, Yang H. Epigallocatechin-3-Gallate protects H(2)O(2)-Induced Nucleus Pulposus Cell apoptosis and inflammation by Inhibiting cGAS/Sting/NLRP3 activation. Drug Des Devel Ther. 2020;14:2113–22.
52. Wang H, Tian Y, Wang J, Phillips KLE, Binch ALA, Dunn S, Cross A, Chiverton N, Zheng Z, Shapiro IM, et al. Inflammatory cytokines induce NOTCH signaling in nucleus pulposus cells: implications in intervertebral disc degeneration. J Biol Chem. 2013;288:16761–74.
53. Huang Y, Mei W, Chen J, Jiang T, Zhou Z, Yin G, Fan J. Gamma-secretase inhibitor suppressed Notch1 intracellular domain combination with p65 and resulted in the inhibition of the NF-κB signaling pathway induced by IL-1β and TNF-α in nucleus pulposus cells. J Cell Biochem. 2019;120:1903–15.
54. Wei R, Chen Y, Zhao Z, Gu Q, Wu J. LncRNA FAM83H-AS1 induces nucleus pulposus cell growth via targeting the notch signaling pathway. J Cell Physiol. 2019;234:22163–71.
55. Zhang X, Qiao B, Hu Z, Ni W, Guo S, Luo G, Zhang H, Ren H, Zou L, Wang P, Shui W. BMP9 promotes the Extracellular Matrix of Nucleus Pulposus cells via inhibition of the Notch Signaling Pathway. DNA Cell Biol. 2019;38:358–66.
56. Rana NA, Haltiwanger RS. Fringe benefits: functional and structural impacts of O-glycosylation on the extracellular domain of notch receptors. Curr Opin Struct Biol. 2011;21:583–9.
57. Chillakuri CR, Sheppard D, Lea SM, Handford PA. Notch receptor-ligand binding and activation: insights from molecular studies. Semin Cell Dev Biol. 2012;23:421–8.
58. Kovall RA, Gebelein B, Sprinzak D, Kopan R. The Canonical Notch Signaling Pathway: structural and biochemical insights into shape, Sugar, and Force. Dev Cell. 2017;41:228–41.
59. Chu D, Zhou Y, Zhang Z, Li Y, Li J, Zheng J, Zhang H, Zhao Q, Wang W, Wang Ra, Ji G. Notch1 expression, which is related to p65 status, is an independent predictor of prognosis in colorectal cancer. Clin Cancer Research: Official J Am Association Cancer Res. 2011;17:5686–94.
60. Hai L, Zhang C, Li T, Zhou X, Liu B, Li S, Zhu M, Lin Y, Yu S, Zhang K, et al. Notch1 is a prognostic factor that is distinctly activated in the classical and proneural subtype of glioblastoma and that promotes glioma cell survival via the NF-κB(p65) pathway. Cell Death Dis. 2018;9:158.
61. Li L, Jin J-H, Liu H-Y, Ma X-F, Wang D-D, Song Y-L, Wang C-Y, Jiang J-Z, Yan G-H, Qin X-Z, Li L-C. Notch1 signaling contributes to TLR4-triggered NF-κB activation in macrophages. Pathol Res Pract. 2022;234:153894.
62. Jin Y, Li C, Xu D, Zhu J, Wei S, Zhong A, Sheng M, Duarte S, Coito AJ, Busuttil RW, et al. Jagged1-mediated myeloid Notch1 signaling activates HSF1/Snail and controls NLRP3 inflammasome activation in liver inflammatory injury. Cell Mol Immunol. 2020;17:1245–56.
63. Liao Z, Ke W, Liu H, Tong B, Wang K, Feng X, Hua W, Wang B, Song Y, Luo R, et al. Vasorin-containing small extracellular vesicles retard intervertebral disc degeneration utilizing an injectable thermoresponsive delivery system. J Nanobiotechnol. 2022;20:420.
64. Zheng Y, Liu C, Ni L, Liu Z, Mirando AJ, Lin J, Saijilafu, Chen D, Hilton MJ, Li B, Chen J. Cell type-specific effects of notch signaling activation on intervertebral discs: implications for intervertebral disc degeneration. J Cell Physiol. 2018;233:5431–40.
65. Liu Z, Chen J, Mirando AJ, Wang C, Zuscik MJ, O'Keefe RJ, Hilton MJ. A dual role for NOTCH signaling in joint cartilage maintenance and osteoarthritis. Sci Signal. 2015;8:ra71.
66. Manzella L, Tirrò E, Pennisi MS, Massimino M, Stella S, Romano C, Vitale SR, Vigneri P. Roles of Interferon Regulatory Factors in chronic myeloid leukemia. Curr Cancer Drug Targets. 2016;16:594–605.
67. Negishi H, Taniguchi T, Yanai H. The Interferon (IFN) Class of cytokines and the IFN Regulatory Factor (IRF) transcription factor family. Cold Spring Harb Perspect Biol. 2018;10.
68. Taniguchi T, Ogasawara K, Takaoka A, Tanaka N. IRF family of transcription factors as regulators of host defense. Annu Rev Immunol. 2001;19:623–55.
69. Sun L, Jiang Z, Acosta-Rodriguez VA, Berger M, Du X, Choi JH, Wang J, Wang K-W, Kilaru GK, Mohawk JA, et al. HCFC2 is needed for IRF1- and

IRF2-dependent Tlr3 transcription and for survival during viral infections. J Exp Med. 2017;214:3263–77.
70. Heinz S, Haehnel V, Karaghiosoff M, Schwarzfischer L, Müller M, Krause SW, Rehli M. Species-specific regulation of toll-like receptor 3 genes in men and mice. J Biol Chem. 2003;278:21502–9.
71. Zhang Y, Zhang Y, Yang A, Xia F. Downregulation of IRF2 alleviates Sepsis-related acute kidney Injury in vitro and in vivo. Drug Des Devel Ther. 2021;15:5123–32.
72. Mohd Isa IL, Teoh SL, Mohd Nor NH, Mokhtar SA. Discogenic low back Pain: anatomy, pathophysiology and treatments of intervertebral disc degeneration. Int J Mol Sci. 2022;24.
73. Ding F, Shao Z-w. Xiong L-m: cell death in intervertebral disc degeneration. Apoptosis. 2013;18:777–85.
74. Zhang X-B, Hu Y-C, Cheng P, Zhou H-Y, Chen X-Y, Wu D, Zhang R-H, Yu D-C, Gao X-D, Shi J-T, et al. Targeted therapy for intervertebral disc degeneration: inhibiting apoptosis is a promising treatment strategy. Int J Med Sci. 2021;18:2799–813.

Publisher's note